Fine-Scale Identifying Archaeological Features Using KH-9 HEXAGON Mapping and Panoramic Camera Images: Evidence from Liangzhu Ancient City

Amir Reza Shahtahmassebi[1], Golnaz Shahtahmassebi[2], Nathan Moore[4], Peter M. Atkinson[5]

[1]*Architectural Engineering School, Hengxing University, Qingdao 266100, China*
[2]*Department of Physics and Mathematics, School of Science and Technology, Nottingham Trent University ,UK*
[3]*Department of Geography, Michigan State University, East Lansing, MI 48823, USA*
[4] *Faculty of Science and Technology, Lancaster University, Bailrigg, Lancaster LA1 4YQ, UK*

*Corresponding authors: amirreza208@hotmail.com;

Fine-Scale Identifying Archaeological Features Using KH-9 HEXAGON Mapping and Panoramic Camera Images: Evidence from Liangzhu Ancient City

Abstract

Historical fine-scale information of archaeological landscapes, such as geometry and spatial patterns is crucial in archaeological investigations. However, documenting such information using satellite sensor data prior to year 2000 remains a daunting challenge. The images from declassified archives of KH-9 HEXAGON (KH-9) cameras including panoramic camera system (PCS) and mapping camera system (MCS) offer fine-scale details of archaeological features. However, noise, contrast distortions and having only a single panchromatic band can tarnish their advantages particularly in identifying such features in subtropical climates with heterogeneous landscape types. This paper focuses on developing a novel multifaceted analytical framework with two components: image pre-processing and feature identification. The image pre-processing component divides into two steps. First, a trained stationary wavelet transforms (SWT) based on the normalised sill (NS) is developed to not only de-noises the image, but also preserves original image characteristics. Then, the contrast of de-noised images is optimised by multi-resolution Top-hat (MTH) using multi-scale information. In the feature identification component, the MCS image is analysed by proposing spatial colour composite write function memory (SCCWFM) and spatial novelty detection (SND). Ultra-fine spatial three-dimensional colour composite (UFSTCC) image and ultra-fine spatial digital surface model (UFSDSM) are devised for interpreting KH-9 PCS images. The proposed pipelines were tested on KH-9 MCS and PCS images of a World Heritage site at the Liangzhu Ancient City (LAC) in China, which is characterised by a subtropical climate with heterogeneous landscape types. The proposed pre-processing pipeline improved considerably the appearance of these images across archaeological landscape types while maintaining original image information. The developed digital analytical approaches for KH-9 PCS and MCS images facilitated straightforward identification of archaeological features in LAC. The multifaceted analytical framework proposed has the potential to increase exploitation of the available KH-9 images in archaeological and cultural heritage applications.

Keywords: KH-9 HEXAGON, Stationary Wavelet Transform, Novelty Detection, Stereo-pairs, Digital Surface Model, Liangzhu Ancient City

1. Introduction

Archives of declassified film-based images of the United States of America (USA) Keyhole (KH) program have been utilized extensively in archaeological research. Such images offer potential advantages: captured four to five decades ago (Casana 2020), fine spatial resolution (Ur 2003), large geographic footprint and stereo-view (Galiatsatos, Donoghue, and Philip 2008). Reviews of applications of KH images in archaeological research have been given by Fowler (2013) , Lasaponara and Masini (2011), Lasaponara et al. (2018) and Luo et al. (2019).

Declassified images from the archives of KH-9 HEXAGON (KH-9), one of the satellite missions of the KH program, offers a unique and irreplaceable source of legacy data for archaeological investigations (Fowler 2016, 2022; Hammer, FitzPatrick, and Ur 2022). The KH-9 mission included two camera systems: mapping camera system (MCS) and panoramic camera system (PCS) (Hammer, FitzPatrick, and Ur 2022). The MCS which had a medium spatial resolution (6 to 9m), captured almost all of the globe (except Greenland, Australia and Antarctica) (Surazakov and Aizen 2010). Despite medium spatial resolution, MCS images can reveal details of archaeological remains (Fowler 2016). Considering overlap characteristics, images of this camera can be used for reconstructing historical digital elevation models (DEMs)(Dehecq et al. 2020; Maurer and Rupper 2015; Surazakov and Aizen 2010). The images from KH-9 MCS were already released in 2002, and they can be downloaded via Earth Explorer as 'Declass 2' (https://earthexplorer.usgs.gov). The PCS composed of ultra fine spatial resolution stereoscopic camera systems (0.6 to 1.2 m) which was integrated in every mission (Marzolff et al. 2022). PCS images have great potential for identifying archaeological features with respect to (i) the ultra-fine spatial resolution, (ii) three-dimensional view and (iii) historical digital surface models (DSM) (Hammer, FitzPatrick, and Ur 2022). The KH-9 PCS images were made available to the public in 2011, but these images have been added into Earth Explorer in 2020, as 'Declass3' (https://earthexplorer.usgs.gov).

Indeed a number of studies have exploited advantages of KH-9 PCS (Fowler 2022) and MCS (Scardozzi 2010) in archaeological research of Near Eastern Regions using visual interpretation. A comprehensive review and demonstrations on these valuable references can be found in Hammer, FitzPatrick, and Ur (2022). Conversely, the use of KH-9 panchromatic images could be challenging particularly under subtropical climate with heterogeneous landscape types (e.g., East Asia)(Watanabe et al. 2017). Arguably, there are three major obstacles: (1) noise, (2) contrast distortions and (3) single panchromatic band. Noise and contrast distortions impede accuracy of both visual interpretation and digital image processing (Shahtahmassebi et al. 2023). Particularly, heterogeneity of landscapes can be increased by noise and contrast distortions in the image. Moreover, identifying archaeological features and their potential marks (e.g., soils and crops) based on a single panchromatic band is a non-trivial task (Fowler and Fowler 2005). For example, surfaces such as vegetation covers, moist soils, water bodies and archaeological features show very similar brightness values in panchromatic imagery, leading to misinterpretation or misclassification problems.

Of particular note that insufficient technical documentations (e.g., articles) and parameters (e.g., Rational Polynomial Coefficient (RPC)) can exacerbate evaluating contemporary pre-processing and feature identification techniques or proposing new frameworks (Dehecq et al. 2020; Marzolff et al. 2022; Maurer and Rupper 2015; Surazakov and Aizen 2010).

The existing state-of-the-art approaches in digital image pre-processing (e.g., wavelet transform and mathematical morphology) (e.g., Bai, Zhou, and Xue 2012; Galiatsatos 2004; Soille 2003) and processing (image matching, structure from motion (SfM)) (e.g., Dehecq et al. 2020; Nita et al. 2018) rely heavily on fine-scale characteristics of the image such as textures, neighbourhoods, spatial, contextual and geometry. In this view, both KH-9 MCS and PCS images offer such characteristics which could be great benefit to those methods.

Given merits and demerits associated with the obsolete film-based panchromatic KH-9 MCS and PCS imagery, five crucial questions arise:

(1) How can appropriate de-noising and contrast enhancement techniques be developed for KH-9 imagery with the least image distortion?
(2) Using KH-9 MCS, how can we effectively establish a spatial colour composite image (for MCS) by leveraging its fine-scale characteristics?
(3) What type of continuous mapping techniques is appropriate for KH-9 MCS?
(4) What type of three-dimensional colour composite approach is effective for KH-9 PCS with respect to its ultra-fine spatial details and lack of technical parameters?
(5) How can we establish ultra-fine scale historical DSM with minimum technical information?

The overarching objective of this research was, thus, to develop a multifaceted analytical framework to identify and map archaeological features in a subtropical climate which is characterised by the heterogeneous landscape types highly heterogeneous, comprising a mixture of archaeological remains, moist soil, vegetation covers, water bodies (such as rivers and ponds) and rural regions, through simultaneous analysing both a pair of KH-9 PCS images in 1975 and a single KH-9 MCS image in 1975. The specific contributions of this research are: (1) a two-step pre-processing pipeline that is devised to both de-noising and optimising contrast of image while preserving and enhancing the salient properties of image objects from KH-9 PCS and MCS, (2) a spatial colour composite write function memory (SCCWFM) that is developed to facilitate identifying features on KH-9 MCS, (3) a spatial novelty detection (SND) that is designed to map spatial distribution of features on KH-9 MCS image, (4) a fully automatic ultra-fine spatial three-dimensional colour composite (UFSTCC) approach based on structure from motion (SfM) algorithm that is proposed to create three dimensional colour composite image using KH-9 PCS, and (5) a fully automatic ultra fine spatial digital surface model (UFSDSM) via SfM that is implemented to establish historical ultra fine-scale DSM. It is noteworthy that contribution No.4 does not need any technical parameters of KH-9 PCS while contribution No. 5 relies on minimum technical parameters (i.e., scanning resolution and focal length).

To assess systematically and comprehensively the outcome of proposed multifaceted analytical approach, we acquired three images from the archives of KH-9. Such images were selected because they covered a heterogeneous archaeological region in wet climate. Moreover, sufficient information was available with which to support our findings.

2. Study area and datasets

2.1.Study area

The study area is Liangzhu Ancient City (LAC) which is located approximately 30 km northwest of the centre of Hangzhou city, Zhejiang Province, China (Figure.1). The study area is classified as a humid climate (subtropical monsoon), with annual rainfall of 1150 to 1550 mm and an average annual temperature of 16 °C (Watanabe et al. 2017). Therefore, this region is highly heterogeneous, comprising the juxtaposition of a mixture of archaeological remains, moist soil, vegetation covers, water bodies (such as rivers and ponds) and rural regions. Ultimately, such surfaces lead to mixed pixels among different land cover types from single panchromatic band. For instance, surfaces such as water, moist soil, archaeological remains and vegetation covers may exhibit very similar values in panchromatic imagery, resulting potential errors in visual interpretation and digital image classification.

It is noteworthy that LAC was for the first time discovered by Shi Xingeng in 1936, and have been studied continuously since that time (Watanabe et al. 2017). LAC is represented by advanced civil engineering systems (such as dams, agricultural systems, palace and waterways), jade ornaments and hierarchical social structure during Liangzhu Culture period (ca. 3300–2500 cal. BC2)(Watanabe et al. 2017). LAC was placed on the United Nations Education, Scientific, and Cultural Organisation’s (UNESCO) world heritage list as a cultural site on July 6, 2019 (Wang et al. 2022). Detailed historical description of the LAC can be found in following references (Wang et al. 2022; Watanabe et al. 2017; Yu et al. 2018).

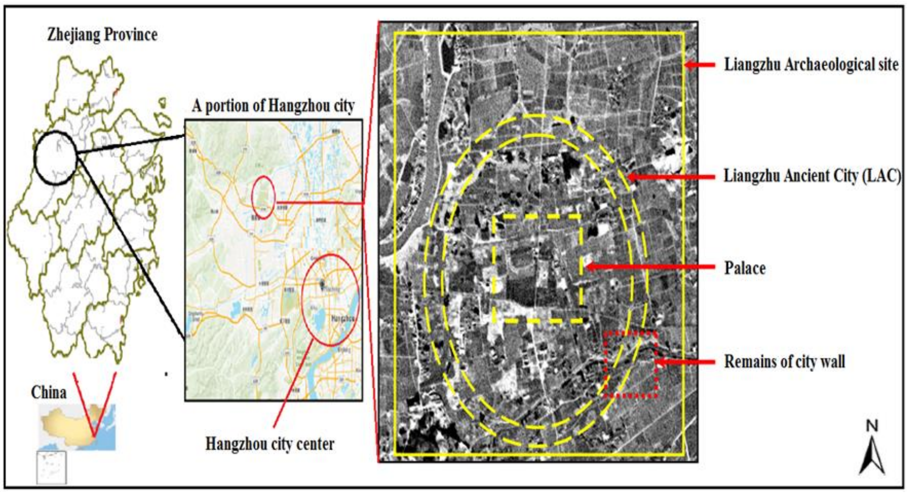

Figure 1. Location of the Liangzhu Ancient City (LAC) in Hangzhou city, Zhejiang Province, China. The coordinate centre of the image is 119°59'2.346" E, 30°23'35.988" N. Our investigation is situated within the large rectangle with the continuous yellow line.

2.2.Datasets

Three KH-9 images over the study area were downloaded via EarthExplorer (http://earthexplorer.usgs.gov) (Table 1).

Table 1. Summary of basic properties of the KH-9 imagery used

Camera	**Date**	**Frame**	**mission**	**tile**	**Spatial resolution(m)**	**Entity ID**
MCS	December 18,1975	7	1211-5	a	6-9m	DZB1211-500049L007001
PCS	August 29,1975	11	1210-3	b	0.6-1.2m	D3C1210-300523F011
PCS	August 29,1975	12	1210-3	i	0.6-1.2m	D3C1210-300523A012

The original images were scanned by in the U.S. Geological Survey (USGS) EROS archive (www.usgs.gov) using high performance photogrammetric film scanners at 7-micron (3,600 dpi). It is noteworthy that the location of samples in LAC was obtained from previous research in the region (Watanabe et al. 2017; Yu et al. 2018) .

Methods

The overall methodology is divided into three parts: pre-processing, KH-9 MCS analytical frameworks and KH-9 PCS analytical frameworks (Figure. 2). The pre-processing included de-noising and contrast enhancement. Both steps were applied to KH-9 MCS and PCS images. The KH-9 MCS image is analysed by proposing spatial colour composite write function memory (SCCWFM) and spatial novelty detection (SND). An ultra-fine spatial three-dimensional colour composite (UFSTCC) image and ultra-fine spatial digital surface model (UFSDSM) are devised for interpreting KH-9 PCS images. These steps were applied to whole study area. Moreover, we take into account devising approaches with two characteristics: less image distortions and semi- or fully- automatic procedures. For the calibration purposes, KH-9 MCS images were initially subjected to the proposed and benchmark pre-processing pipelines. Then, the KH-9 MCS and PCS images were pre-processed by the selected pre-processing technique.

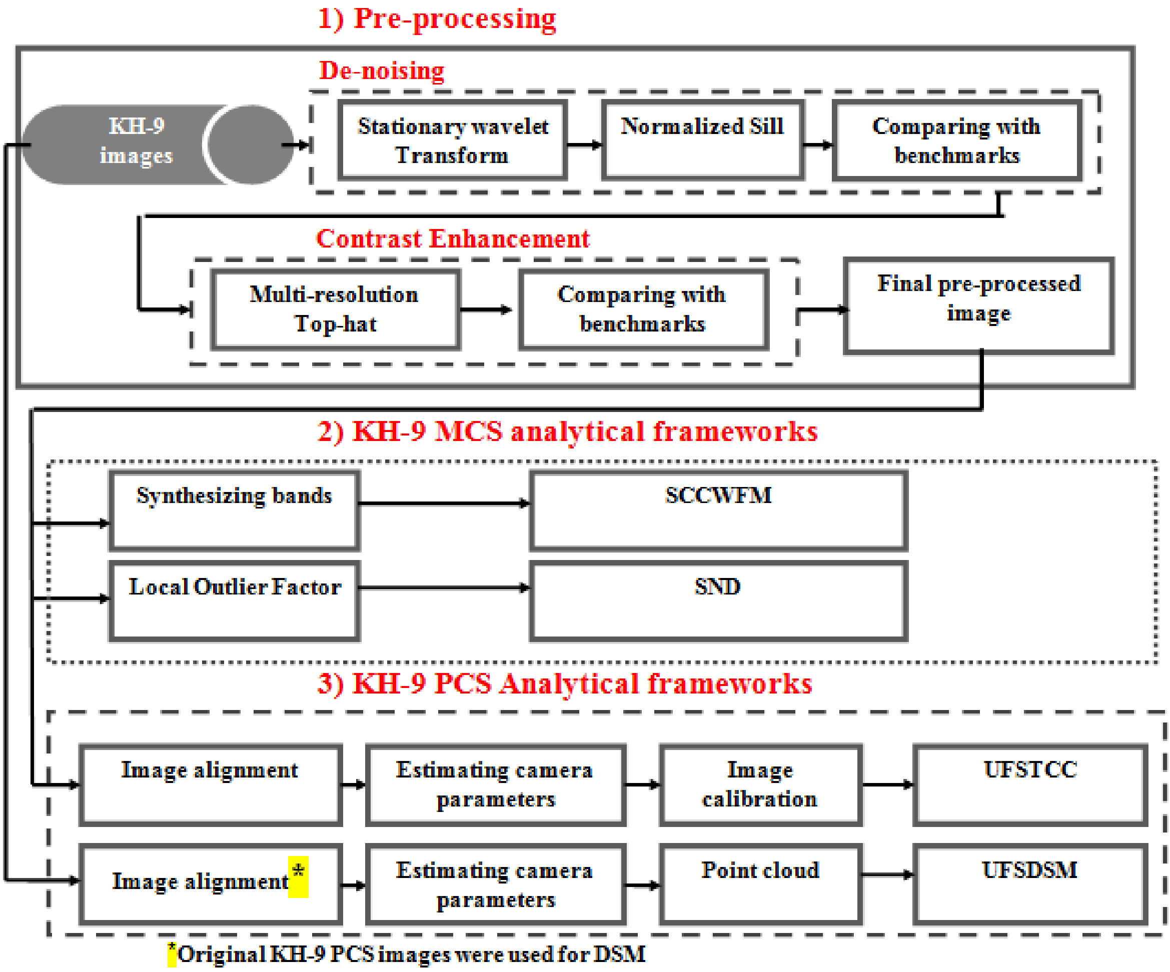

Figure 2. Research workflow. The KH-9 MCS image is analysed by proposing spatial colour composite write function memory (SCCWFM) and spatial novelty detection (SND). Ultra fine spatial three-dimensional colour composite (UFSTCC) image and ultra fine spatial digital surface model (UFSDSM) are devised for interpreting KH-9 PCS images.

2.3. Image pre-processing

In order to minimize effects of noise and contrast degradation, this research adopted de-noising and contrast enhancement pipeline for KH-9 image proposed by Shahtahmassebi et al. (2023). In this pipeline, image de-noising was done by stationary wavelet transform (SWT) while multi-resolution Top-hat (MTH) is used to optimize contrast of the image. Besides evaluating performance of this pipeline for using KH-9 images in archaeological investigations, our research improved this pipeline in four aspects, which are as follows:

(1) Selecting SWT directional coefficients using a geostatistical approach

One of the major concerns in SWT de-noising procedure is selecting appropriate wavelet directional coefficients so as to avoid over-smoothing or loss of contrast. Conventional image quality assessment approaches, such as the Peak Signal-to-Noise Ratio (PSNR), may not be appropriate as they are not sensitive enough to local spatial variation of image brightness values. However, geostatitical techniques such as semivariogram are based on local spatial information which can capture precisely the change in local spatial variation of the image.

Semivariogm analysis consists of several parameters, such as the sill and range, which generate interpretable information about local spatial structure within the image. Of these parameters, sill in semivariogram analysis is a valuable tool to quantify impacts of wavelet directional coefficients on the image and, thus, assessing performance of de-noising. This is because the sill represents the magnitude of the structured component of the variance. We therefore assumed that any degradation in local spatial variation of brightness values due to selecting inappropriate wavelet directional coefficients can be reflected in the sill of semivariograms. Accordingly, distortions in spatial variation of brightness values can be quantified by the difference between the sill of the original image and the sill of the de-noised image, called the normalized sill (NS):

$$\text{Normalized Sill} = \frac{\text{Sill}_{\text{De-noised}} - \text{Sill}_{\text{Original image}}}{\text{Sill}_{\text{De-noised}} + \text{Sill}_{\text{Original image}}} \quad (1)$$

The SWT de-noising steps were as follows:

(i) Decomposition: The Haar mother wavelet was selected to decompose image into vertical, horizontal and diagonal directions. The Haar was computed empirically at three levels.

(ii) De-noising: A range of directional coefficient values with a 10-unit increment were selected empirically. This range was divided into seven groups with values from four (less image distortion and more noise) to 58 (high degree of over-smoothing and less noise). The coefficients along with soft thresholding techniques were used to generate de-noise images (seven images).

(iii) Normalized sill (NS): Semivariogram analysis was applied to all de-noised images and the original image. In order to apply semivarogram to the image (a regular matrix), we used global spatial statistics function in RSI ENVI 5.1 (Harris Geospatial Solutions$^{\text{TM}}$). The semivariogram was calculated with a maximum lag distance of 21 pixels and using the Queen's case as the neighbourhood rule (considering all eight neighbouring pixels). However, this function does not extract semivariogram parameters. Hence, the computed semivariograms in ENVI were imported to "geostat library" of the R-language to calculate semivariogram parameters. The obtained sills were then subjected to NS procedure (equation No.1).

Considering de-noising procedure needs to adjust some parameters, this procedure was conducted semi-automatically. The proposed framework integrates the Stationary Wavelet Transform (SWT) and normalized sill, hence, this framework is abbreviated to SWTNS.

(2) Benchmark de-noising techniques

In order to examine effectiveness of the proposed de-noising step, we used four advanced benchmark methods (Dictionary learning, Total Variation, Shift invariant wavelet and Non-local means filtering (NLMF)) which are based on the local spatial information. The Dictionary learning was established by using orthogonal matching pursuit (OMP), two non-zero coefficients and patch size of 7×7. The random noise function was employed to generate a distorted image for training procedure.

For Shift invariant wavelet, cycle spinning technique was designed through three steps: circularly, de-noising and inverse shift. It is noteworthy that we tested a range of max_shifts, consisting of 1,2,3,4 and 5. A shift_max of 5 was found empirically to be appropriate for de-noising. With respect to Total Variation, we examined a range of de-noising weight, including 0.1, 0.2, 0.3, 0.4 and 0.5, and 0.2 was found to be optimal for removing the noise with least image degradation.

Furthermore, Non-local means filtering (NLMF) was implemented to remove effects of noise. In this research, we found that pre-define parameters of this filter to be optimal for de-noising with least image distortion. NLMF was implemented in Matlab® (MathWorks Inc., Natrick, MA, USA. Release:2018b) while the rest of benchmark techniques were computed in Python. These benchmarks were conducted fully automatically.

(3) Benchmark contrast enhancement techniques

The proposed multi-resolution Top-hat (MTH) uses local spatial and neighbourhood information to optimize contrast of the image. In order to understand comprehensively and systematically the performance of this technique, we adopted Fast Local Laplacian filtering (FLLF) which employs local spatial information. FLLF was computed in Matlab® (MathWorks Inc., Natrick, MA, USA. Release:2018b). Further details of MTH and setting parameters for KH-9 images can be found in Shahtahmassebi et al. (2023).

(4) Image quality assessment strategy

To assess effects of pre-processing on KH-9 images, Gray Level Co-occurrence Matrix (GLCM) measures were employed as they are sensitive to spatial structure of image brightness values (Hall-Beyer 2017). Four gray-level co-occurrence measures were employed: contrast (indicator of local variations), variance (measure of spatial variation), entropy (indicator of the disorder) and homogeneity (measure of distribution in the pixel pairs population). Then standard deviation value for each texture was computed.

Two experimental images were generated separately by adding noise (15%) and blurriness (using Gaussian low pass filter with window size 13×13) to analyse de-noising performance. For contrast enhancement assessment, two additional experimental images were also synthesized: low contrast image using linear enhancement (brightness values between 21 and 242) and high contrast using Gaussian function (brightness values from 16 to 242).

3.2.KH-9 MCS analytical frameworks

3.2.1. Spatial colour composite write function memory (SCCWFM)

A simple yet efficient approach for visual interpretation is write function memory (WFM) (Jensen 2005; Mather and Koch 2004). In effect, each band (or processed product) from multi-spectral remotely sensed data may be placed into each of the three WFM bands (Red-Green-Blue (RGB)) to generate a colour composite image. However, WFM may not be applicable for panchromatic imagery due to its single spectral band. Considering that the boundaries and details of archaeological remains have a key role in their identification, we assume that generating new bands sensitive to spatial information and placing them in WFM may facilitate the identification of archaeological features from KH-9 MCS images.

In this research, a WFM was constructed using a directional filter, GLCM-mean measure and a Sobel edge detector filter. The directional filter is a first derivative edge enhancement filter that selectively enhances image features with specific directional components (gradients) and window size. The directional filter was calculated at an angle of 45° and window size of 3×3 pixels. A Sobel edge detector is a non-linear edge enhancement which detects edges of image objects. The GLCM-mean measure is the average gray-level in the local window with respect to the neighbourhoods. This measure was calculated using a window size of 3×3 pixels. This was performed to further reduce the effects of potential unnecessary brightness anomalies while detecting sharp spatial variation in the image occurring in the boundaries of human-made features and non-human-made features. Finally, directional filter, GLCM-mean and Sobel filter were placed as Red, Green and Blue bands in WFM, respectively.

3.2.1. Spatial novelty detection (SND)

In order to produce spatial map of potential archaeological remains, we utilized novelty detection approach in this research. Novelty detection techniques reveal new outlier/anomaly patterns in unseen datasets. This research assumed that change in brightness values of non-archaeological surfaces could be different from archaeological landscapes. Hence, if training samples collected from non-archaeological regions, with subtle and gradual change in contrast, is then compared to that of an unknown site (supposed archaeological sites), new or novel pattern can be revealed on the unknown region. To this end, the Local Outlier Factor (LOF) algorithm, which is an unsupervised novelty detection method, was adopted for this research (Breunig et al. 2000). The strength of the LOF algorithm is that it takes both local and global properties of datasets into consideration. This advantage is explained by the local aspect of LOF, meaning that it only compares the score of abnormality of one sample with the scores of its neighbours (Pedregosa et al. 2011).

In this research, LOF procedure was as follows: sampling, training and modelling. Firstly, we collected several sample points from non-archaeological features which were located outside of LAC region. All the training samples characterize by gradual or subtle change in brightness values. The land use and land cover map of the region was also employed for identification procedure; Secondly, LOF model was trained using collected training samples. Then the image over LAC region was subjected to the established LOF model. In LOF, the numbers of neighbourhood and contamination were defined as 25 and 0.5, respectively.

Prior to applying LOF to whole study area, we initially built a LOF model using collected archaeological and non-archaeological samples. The results showed that although there was high pixel confusion between archaeological and non-archaeological samples on the KH-9 MCS image, LOF can enable us to identify pixels in archaeological samples from those in non-archaeological regions (Figure.3). Therefore, the proposed LOF model was applied to whole study area.

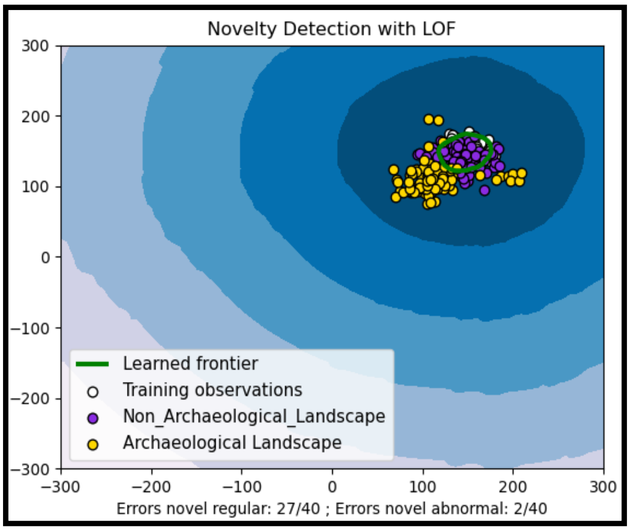

Figure.3. Applying LOF to archaeological and non-archaeological samples

*3.3. **KH-9 PCS analytical frameworks***

3.3.1. Ultra fine spatial three-dimensional colour composite (UFSTCC)

In general, creating accurate stereo-pairs rely on camera calibration parameters (e.g. RSI ENVI). In the case of KH-9 PCS camera, such parameters have yet to be released. Stereo pairs can be therefore done manually (without camera parameters) in some software (e.g., ERDAS Imagine). However, screen digitizing is time-consuming and complex. In order to generate accurate geo-rectified stereo-pairs, we employed the fully automatic stereo-pairs rectification algorithm for uncalibrated cameras. This algorithm included five major steps (Shahtahmassebi et al. 2023): (1) two images were aligned based on matching pixels between two images. The alignment procedure used a Speeded-Up Robust Features (SURF) approach for matching pixels on two images. The extracted pixels were then compared by sum of absolute differences indicator to identify strong matching pixels in both images; (2) selected matching pixels were examined by random sample consensus (RANSAC) in order to satisfy the epipolar constraint; (3) the final pixels were used to estimate fundamental matrix; (4) two images were rectified using the parameters in fundamental matrix; and (5) the rectified images were placed into in stereo anaglyph system to create stereo-pairs image. The image stereo-pairs were performed fully automatically in Matlab® (MathWorks Inc., Natrick, MA, USA. Release:2021b). The whole procedures took approximately 20 minutes.

3.3.2. Ultra fine spatial digital surface model (UFSDSM)

Creating DSM could be challenging using stereo-pairs from KH archives such as KH-9 and KH-4B (CORONA) due to unknown camera parameters, identifying accurate ground control points (GCP), earth curvature, software problems (e.g., bowl effect), change in landscape, acquiring fine spatial resolution reference DEM and errors in estimating camera parameters (Watanabe et al. 2017). In addition, reconstructing DSM over planar surface (flat) using these data may not offer promising results (Maurer and Rupper 2015) . Considering these problems, herein we aimed to evaluate whether establishing DSM based on KH-9 PCS can identify any archaeological structures in LAC. To this end, we exploited advantages of automatic DSM procedures in Photoscan (Agisoft). In the first step, we used aligning procedure in this software to align two images from KH-9 PCS. The alignment was conducted using information from neighbouring pixels rather than geometric transformation. Second, the tie points were extracted from aligned images. Third, the extracted tie points were used to estimate the intrinsic camera parameters. Fourth, we computed three-dimensional points cloud based on the derived tie points and estimate camera parameters. Finally, the point cloud was used to create a DSM over study area. It is noteworthy that we applied this framework to the original and pre-processed KH-9 PCS images yet, we did not observe any significant differences. Hence, the original images were used for DSM procedure.

4. Results

4.1. Pre-processing

4.1.1. Calibration

In order to understand carefully the performance of different pre-processing techniques, we firstly applied pre-processing techniques to KH-9 MCS image as it had high amount of contrast distortions and noise compared to PCS image. After exhaustive and rigorous assessment, the selected pre-processing methods were applied to both MCS and PCS images.

4.1.2 Identifying appropriate wavelet de-noised image:

We found that increasing the wavelet directional coefficients led to increasingly blurriness, thus, loss of contrast as observed through a sharp decline in the shape of semivariogram, sill and normalized sill (NS) (Figure.4 and Table 2). For instance, applying wavelet coefficient values in the Group_7 (highest values) led to high blurriness (Figure. 4(c)). This phenomenon reflected in sharp decline of sill and NS which implied a decrease in spatial heterogeneity and potential loss of contrast (Figure.4(a) and Table 2). The results of NS and semivariogram analysis along with exhaustive visual inspections demonstrated that the directional coefficients in Group 2 not only eliminated the noise, but also preserved the original image information (Figure. 4(b)). Therefore, the de-noised image based on the wavelet coefficients in the Group_2 was selected for subsequent procedure.

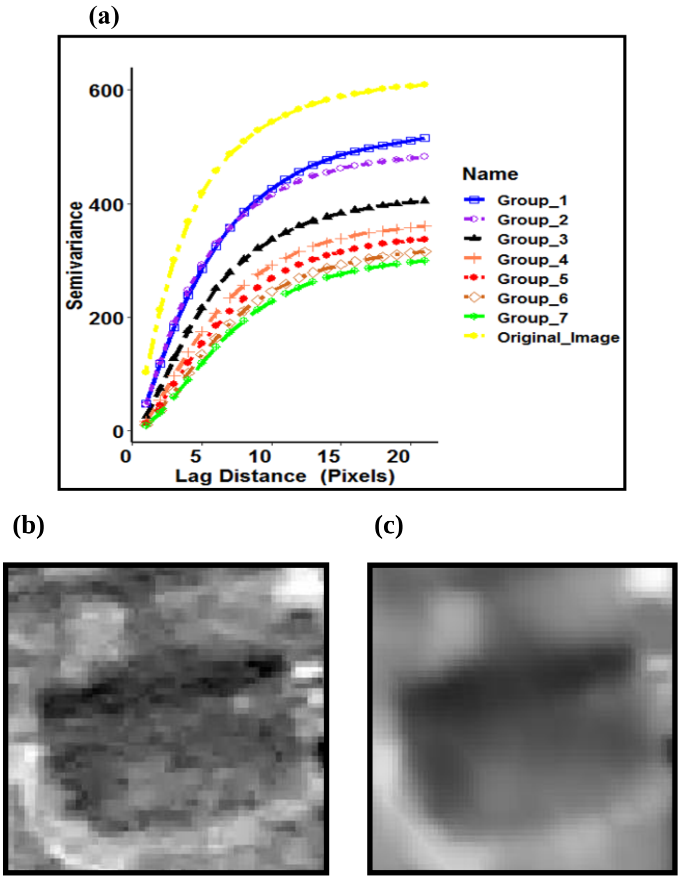

Figure 4. (a) Semivariogram of de-noising images; (b) and (c) show two examples of de-noised images based on wavelet coefficient values in Group_2 and Group_7, respectively. Semivariogram and wavelet were calculated based on the KH-9 MCS image in the calibration step. The coordinate centre of the image (b) and (c) is 30°23′45″ N, 119°59′12″ E. The approximate spatial resolution of these images 6-9m

Table 2 Parameters of the fitted semivariogram

De-noised Group	Model(s)	Nugget	Sill	NS	Range
Original _Image	EXP,MAT	16.47	609.3	---	5.11
Group_1	EXP,MAT	27.85	515.25	-0.08	6.81
Group_2	**EXP,MAT**	**0.0**	**495.5**	**-0.10**	**5.68**
Group_3	EXP,MAT	0.0	415.3	-0.18	6.24
Group_4	EXP,MAT	0.0	379.99	-0.23	6.81
Group_5	EXP,MAT	0.0	364.61	-0.25	7.38
Group_6	Cubic	17.04	289.74	-0.35	19.86
Group_7	**Cubic**	**16.15**	**274.53**	**-.37**	**19.3**

a) De-noising

Figure.6 presents two sample areas of archaeological remains (which were discovered in previous studies; (Watanabe et al. 2017; Yu et al. 2018) in the original KH-9 MCS image, and the result of de-noising using the proposed SWTNS and benchmark techniques. The original KH-9 MCS image was noisy and unclear (Figure.5(a) and Figure.6(I)). The result indicates that the effects of noise can be minimized by de-noising techniques (Figure.5 and Figure.6). In particular, advances in image pre-processing techniques such as proposed SWTNS, dictionary learning and total variation generated appropriate outcomes in comparison to original image and NLMF, as evidenced in image histogram (Figure. 7).

The impact of de-noising on the image quality and spatial properties of the KH-9 MCS image were also assessed by GLCM measures (Table 3). For instance, considering blurred and noisy (15%) images as benchmark levels, variance, representing micro-scale variation of brightness values (BVs), decreased after applying the de-noising techniques. This illustrated that the noise (or potential error) in the original KH-9 image was reduced by applying de-noising techniques (Table3 and Figure.7). Similarly, the contrast, representing the spatial frequency of BVs, decreased slightly after de-noising. However, homogeneity (measure of smoothness) and entropy (indicator of roughness or disorderliness) increased sharply.

Regarding selecting appropriate methods, the results showed that NLMF led to an increase in the variance and contrast which could be due existing potential noise in the de-noised image (Table 3 and Figure.7). In contrast, Total Variation, Shift invariant, Dictionary learning and the proposed SWTNS method reduced the effects of the noise in the KH-9 MCS image as shown by the decreasing contrast and variance (Table 3), and image histogram (Fig. 7). However, image blurriness (smoothness) in the images produced by Total variation and Dictionary learning was large which was reflected in a sharp decline in the variance and contrast, and an increase in entropy and homogeneity. SWTNR and Shift invariant preserved the spatial structure of the KH-9 image yet, Shift invariant generated smaller entropy compared to the SWTNR, potentially due to the existence of noise (Table 3, Figure. 5 and Figure.6). Hence, we suggest that SWTNR may be an appropriate candidate for de-noising KH-9 image.

(x) Original image

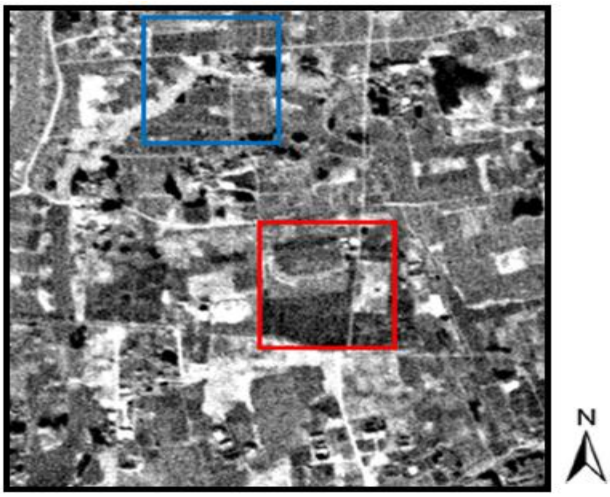

(a) Original image **(b) NLMF** **(c) Total Variation**

(d) Shift invariant **(e) Dictionary learning** **(f) SWTNR**

Figure.5. (x) location of two sample regions on the original image and (a-f) comparison between original image and de-noising techniques using the first sample. The proposed and benchmark methods were applied initially to the KH-9 MCS image in the calibration step. The coordinate centre of the image (X) and image with red rectangle is 30°23′45″ N, 119°59′12″ E. The approximate spatial resolution of these images 6-9m

I. Original image **II. NLMF** **III. Total Variation**

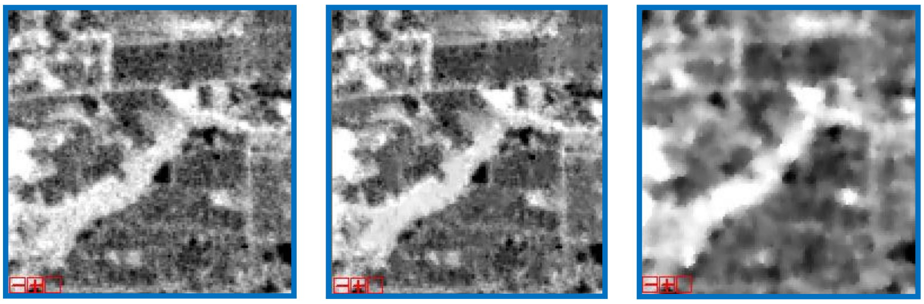

IV. **Shift invariant** V. **Dictionary learning** VI. **SWTNR**

Figure 6. Comparison between original image and de-noising techniques using the second sample from **Figure 5(x)**. The proposed and benchmark methods were applied initially to the KH-9 MCS image in the calibration step. The coordinate centre of the image with blue rectangle is 30°24′05″ N, 119°59′04″ E. The approximate spatial resolution of these images is 6-9m.

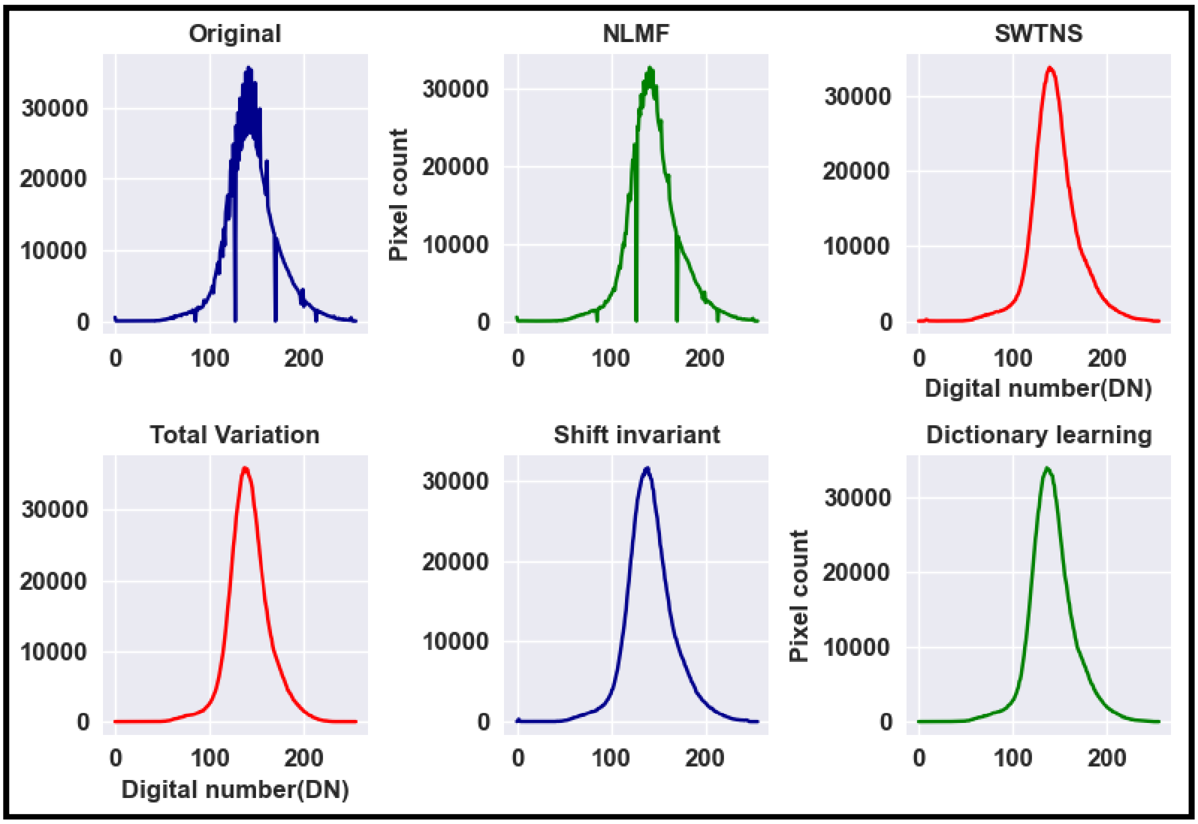

Figure 7. Comparison between image histograms of the de-noised and original images. The proposed and benchmark methods were applied initially to the KH-9 MCS image in the calibration step

Table 3. Standard deviation of GLCM measures before and after de-nosing

b) Contrast enhancement

De-nosing approach	**Variance**	**Homogeneity**	**Contrast**	**Entropy**
Noisy (15%)	46.517950	0.066027	106.510573	0.152998
Gaussian_Blurred	3.695500	0.251967	6.795495	0.464423
Original	**11.218508**	**0.121125**	**19.848635**	**0.182292**
NLMF	11.504236	0.164685	20.455831	0.246257
Total Variation	6.335427	0.216347	11.456247	0.387531
Shift variance	10.278104	0.152264	18.166018	0.231190
SWTNS	**9.893998**	**0.202737**	**17.500872**	**0.354283**
Dictionary	5.838528	0.228053	9.894329	0.378910

The proposed MTH and the FLLF techniques were applied separately to the SWTNS result. Qualitative assessment indicated that the contrast enhancement techniques enhanced the appearance of the original KH-9 image (Figure. 8). For example, the edges of potential archaeological features (Figure.8 (b) and (c)) can be highlighted easily whereas these edges were not readily observable in the original image (Figure.8 (a)). This clearly accentuated the need to optimize the contrast of the original image. Of the contrast enhancement approaches, MTH outperformed the FLLF technique and the original image by achieving the reliable image visual appearance (Figure.8(c)). The image produced by the MTH achieved an appropriate balance between bright and dark BVs. The image also presented archaeological features with the most well-defined details.

Table 4 shows that quantitative assessment supports the results of visual comparison. Considering benchmark images, increasing brightness led to low variance, homogeneity, contrast and entropy while increasing darkness generated inverse results. Having these in mind, the MTH approach enhanced the brightness values of the original KH-9 image homogeneously whereas FLFF algorithm led to a spatially imbalance enhancement. This phenomenon is mirrored in the comparison between GLCM measures (Table 4) and the corresponding image (Figure. 8). For instance, FLFF generated large brightness anomaly which is evidenced by an increase in variance and contrast except entropy. However, MTH optimized brightness of KH-9 MCS image as shown by a decline in those values and visual interpretation. Also, it increased entropy which reflected increase amount of information. The imbalanced enhancement was observed for FLLF which could be partly due to the lack of semantic understanding of the scene (Aubry et al. 2014).

(I) SWTNR-MTH

(a) Original image **(b) SWTNR-FLLF** **(c) SWTNR-MTH**

Figure 8. Results of contrast enhancement; (I) locations of a sample on SWTNR-MTH and (a-c) comparison between original image and proposed contrast enhancement techniques. The proposed and benchmark methods were applied initially to the KH-9 MCS image in the calibration step. The coordinate centre of the image (X) and image with red rectangle is 30°23′45″ N, 119°59′12″ E. The approximate spatial resolution of these images is 6-9m.

Table 4. Standard deviation of GLCM measures before and after contrast enhancement

Contrast enhancement approaches	**Variance**	**Homogeneity**	**Contrast**	**Entropy**
Low contrast	10.566116	0.201060	18.344784	0.339922
High contrast	26.991171	0.184408	44.908942	0.300652
Original	**11.218508**	**0.121125**	**19.848635**	**0.182292**
SWTNR-MTH	**7.474793**	**0.211266**	**13.405540**	**0.430503**
SWTNR -FLLF	12.207025	0.162090	21.233692	0.263666

4.1.3. Pre-processing of KH-9 MCS and PCS using proposed SWTNR-MTH pipeline

The proposed SWT-MTH pipeline was applied to KH-9 MCS and PCS images. Image comparison suggested that the proposed SWTNR-MTH pipeline enhanced the visual appearance of the KH-9 images substantially over the study area (Figure.9 and Figure.10). More importantly, the fine scale details of archaeological features (e.g., edges and geometry) can be identified readily (Figure.9 and Figure.10). For example, one can observe clearly remains of LAC components such as palace and wall in the result of the SWTNR-MTH pipeline. However, such information was not readily observable in the original images (Figure.9 and Figure.10). Moreover, the results indicated that stereo images based on pre-processed KH-9 PCS images revealed greater information in comparison to those based on the original images (Figure.9).

(a) Original KH-9 PCS, sample 1, 1975 **(b) Pre-processed KH-9 PCS, sample 1, 1975**

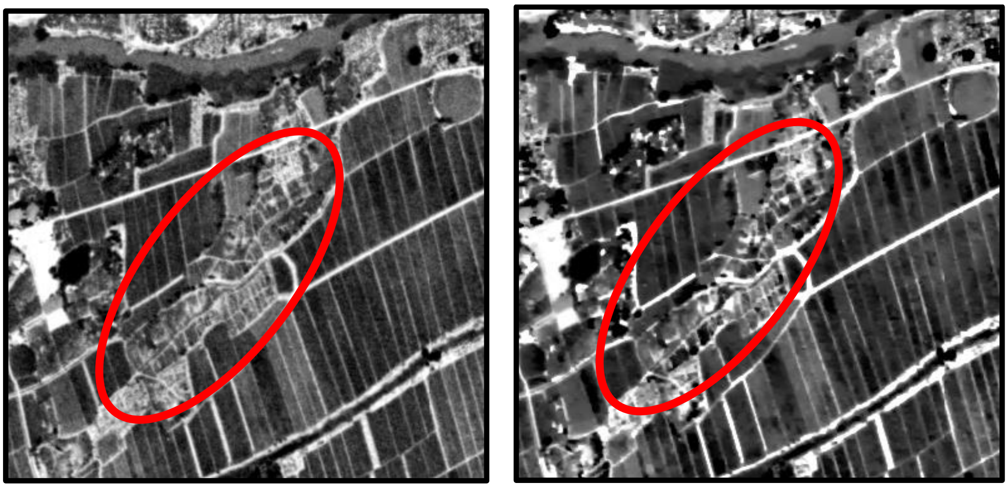

(c) Sample 2 **(d) Sample 2**

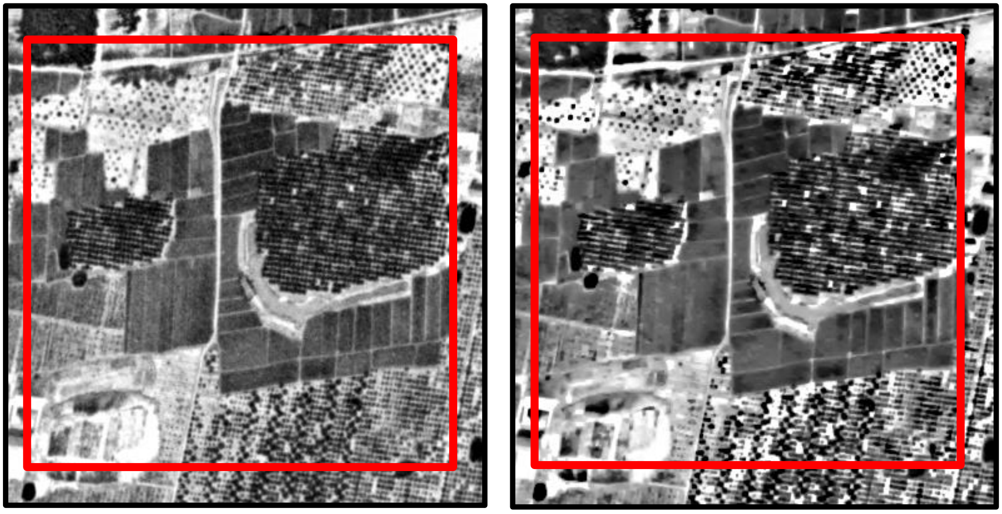

(e) Sample 3 **(f) Sample 3**

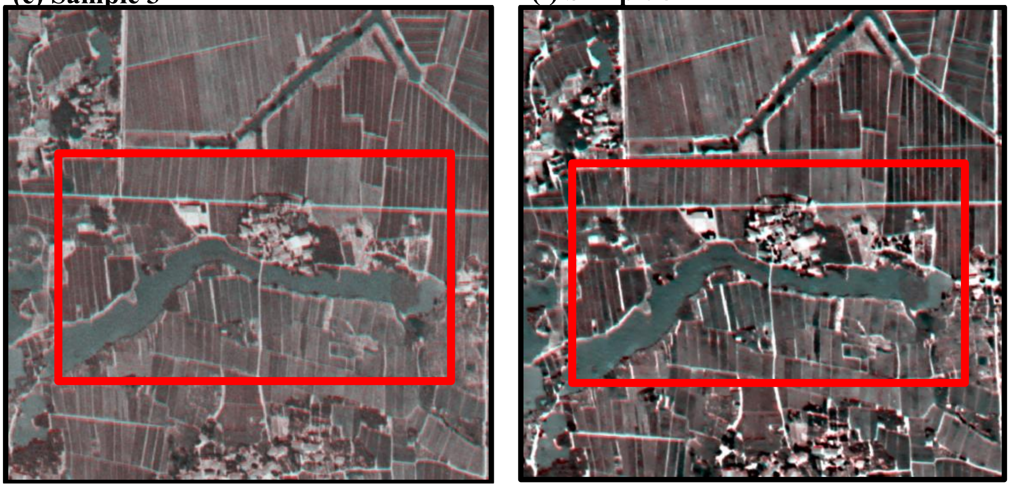

Figure 9. Comparison between archaeological landscapes on original and pre-processed KH-9 PCS images; (a-d) grey scale images and (e-f) stereo-pairs; Samples 1 and 3 represent of remains of wall while sample 2 represents remains of main palace. The coordinate centre of sample 1, 2 and 3 is 30°23′18″ N, 119°59′40″ E; 30°23′45″ N, 119°59′12″ E; and 30°24′05″ N, 119°59′04″ E. The approximate spatial resolution of these images is 0.6-1.8m.

(a) Original KH-9 MCS, sample 1, 1975 **(b) Pre-processed KH-9 MCS, sample 1, 1975**

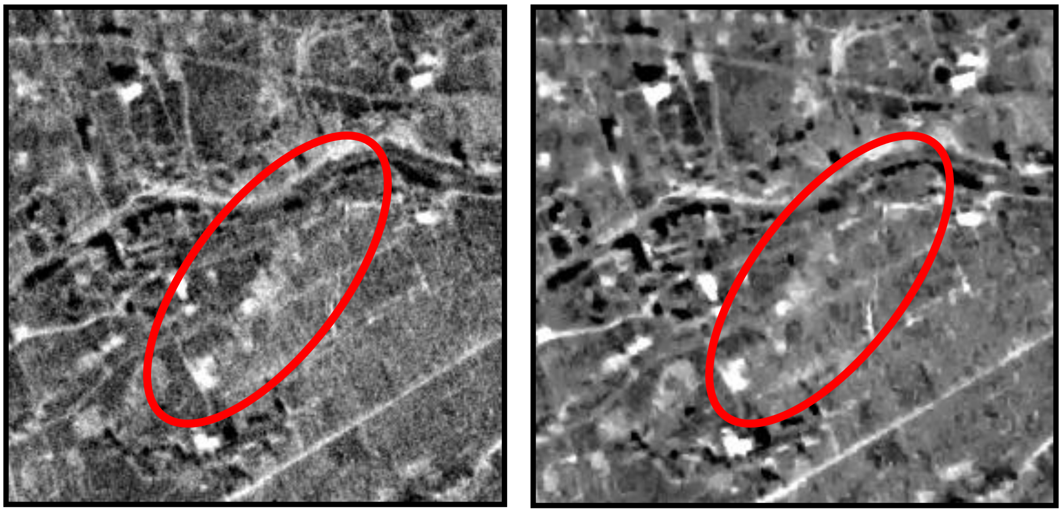

(c) Sample 2 **(d) Sample 2**

(e) Sample 3 **(f) Sample 3**

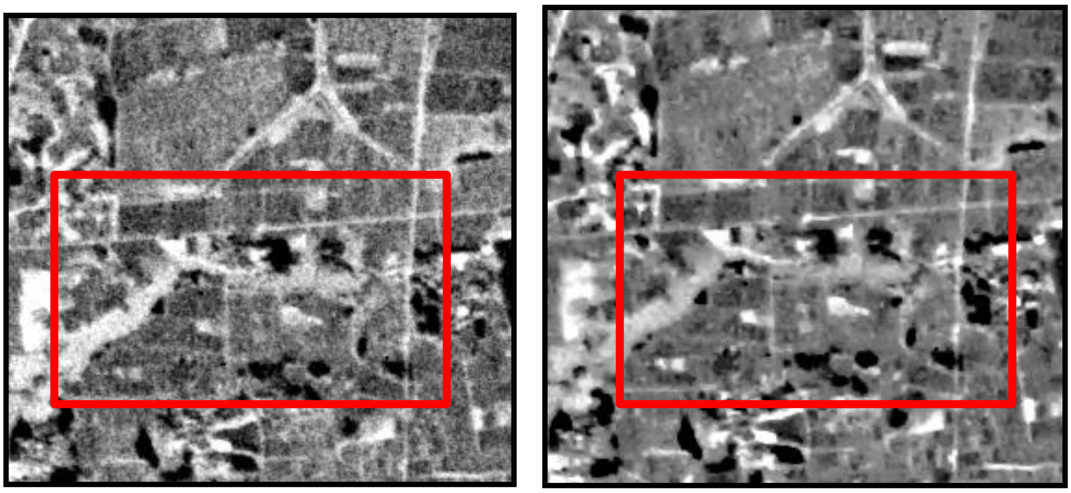

Figure 10. Comparison between archaeological landscapes on original and pre-processed KH-9 MCS images; Samples1 and 3 represent of remains of wall while sample 2 represents remains of main palace. The coordinate centre of sample 1, 2 and 3 is 30°23′18″ N, 119°59′40″ E; 30°23′45″ N, 119°59′12″ E; and 30°24′05″ N, 119°59′04″ E. The approximate spatial resolution of these images is 6-9m.

4.2. KH-9 MCS analytical approaches

SCCWFM illustrated highly complex and heterogeneous landscape in LAC, comprising juxtaposition of a mixture geometric pattern anomalies and natural surfaces (Fig.11). Most archaeological features in this region can be identified by highly fluctuations in colour, pattern and shape (Figure.11). Abnormal changes in contrast were captured by the means of SND (Figure.12). To facilitate investigation, we overlaid the novelty image on the original image. One can see that non-archaeological features were generally located on the regions with constant brightness or subtle change in brightness variations. However, archaeological features were captured in abnormal transition of brightness, as evidenced in the result of SND (Figure. 12). Moreover, the proposed SND result provided outlier values in which lower values (less than -5) not only indicated sharp changes in brightness, but also it may represent high potential of existing archaeological features. It is noteworthy that observed information on SCCWFM and SND provided information data in comparison to the original KH-9 MCS image (Figure. 13).

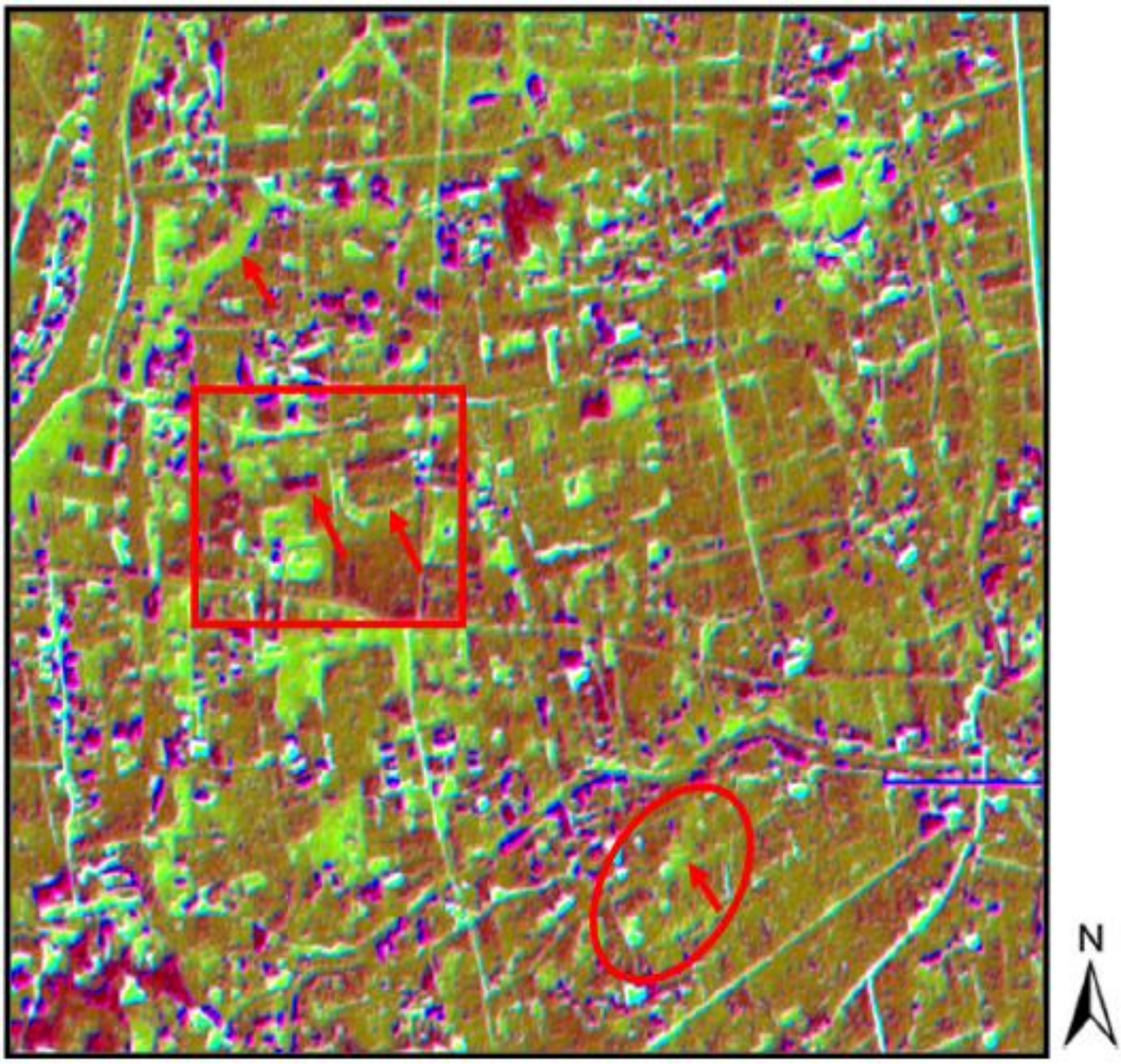

Figure 11. Generated SCCWFM colour composite system over LAC using a panchromatic KH-9 MCS image. The red square, ellipse and arrows show representative archaeological sites. The coordinate centre of the image is 30°23′45″ N, 119°59′12″ E. The approximate spatial resolution of this image is 6-9m.

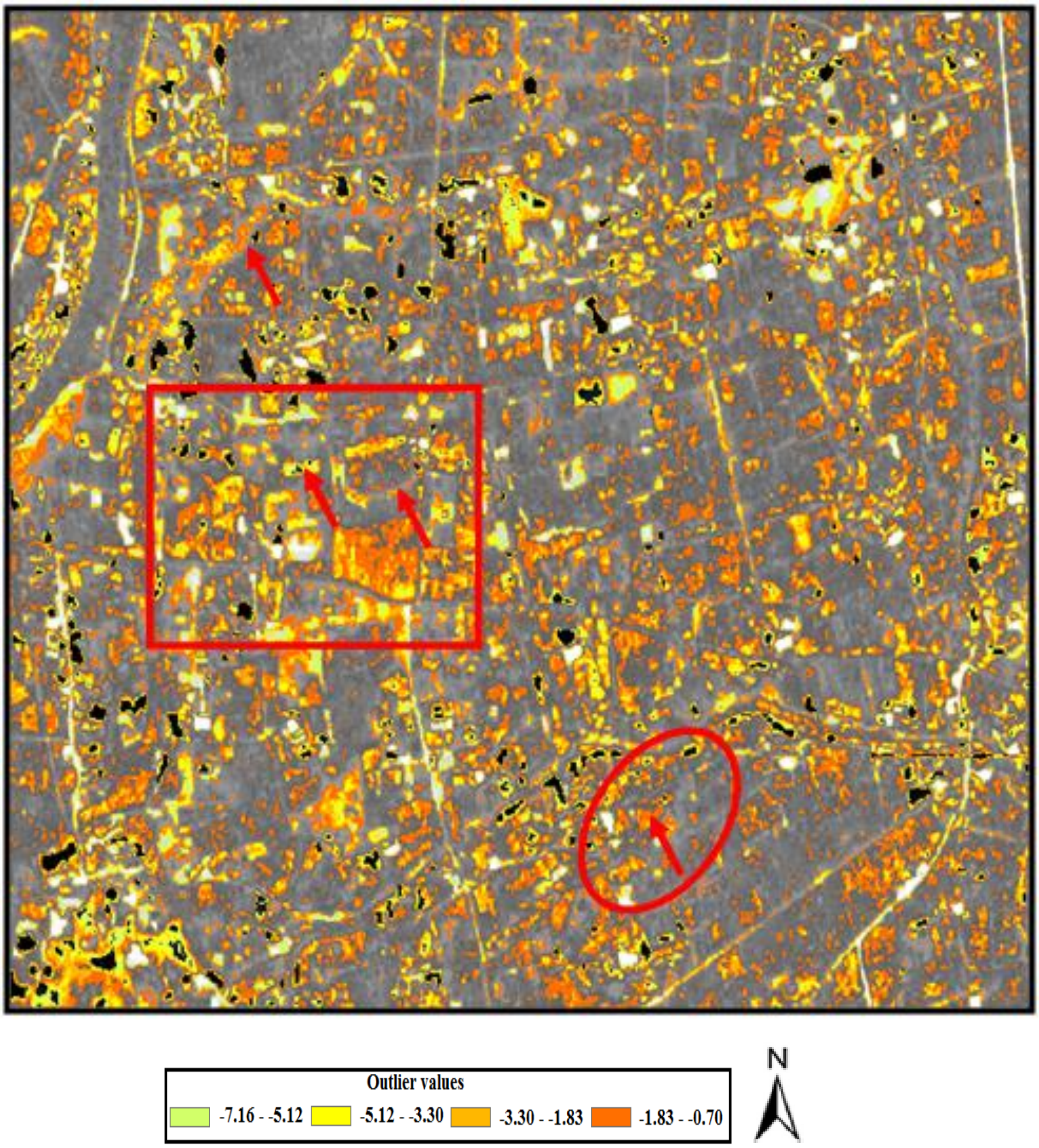

Figure 12. Generated SND based on the panchromatic KH-9 MCS image over LAC. The red square, ellipse and arrows show representative archaeological sites. The coordinate centre of the image is 30°23′45″ N, 119°59′12″ E. The approximate spatial resolution of this image is 6-9m.

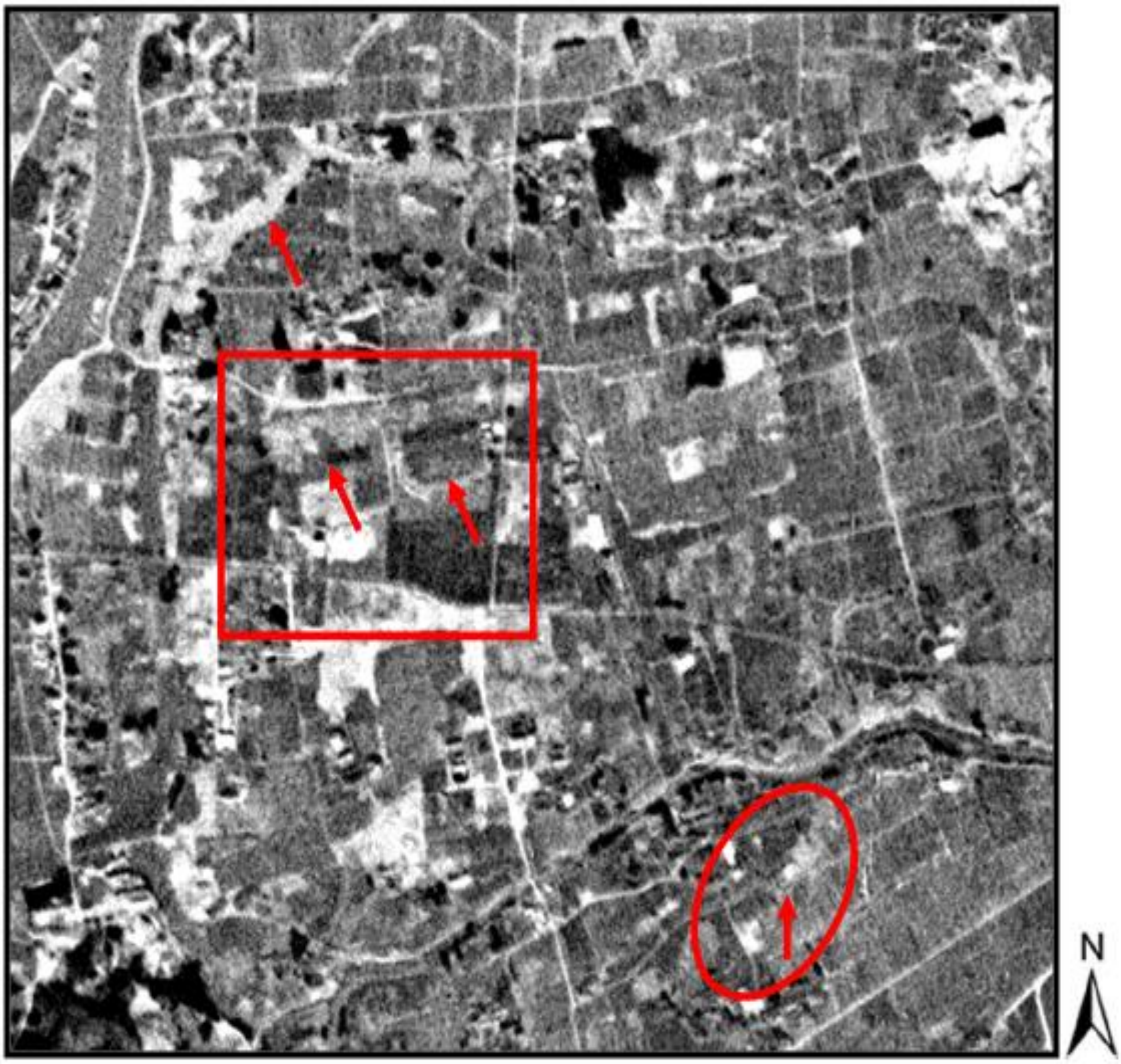

Figure 13. KH-9 MCS original image over LAC. The red square, ellipse and arrows show representative archaeological sites. The coordinate centre of the image is 30°23′45″ N, 119°59′12″ E. The approximate spatial resolution of this image is 6-9m.

4.3.KH-9 PCS analytical frameworks

Fig.14 shows generated three-dimensional colour composite by UFSTCC over LAC. This image offered ultra fine-scale details of the LAC. Accordingly, many archaeological features indicated high degree of shape and colour variation while non-archaeological regions such as agricultural areas indicated homogeneous surface. In addition, we created the DSM of LAC using proposed UFSDSM (Fig.15). Indeed, the estimated DSM not only confirmed existence of the archaeological remains, but also it revealed their structures such as the main palace. Although original image of KH-9 PCS can be useful (Figure.16), the results of UFSTCC and UFSDSM could enhance substantially identification of archaeological remains in the LAC.

Figure 14. The outcomes of UFSTCC over LAC. The yellow square, ellipse and arrows show representative archaeological sites. The coordinate centre of the image is 30°23′45″ N, 119°59′12″ E. The approximate spatial resolution of this image is 0.6-1.8m.

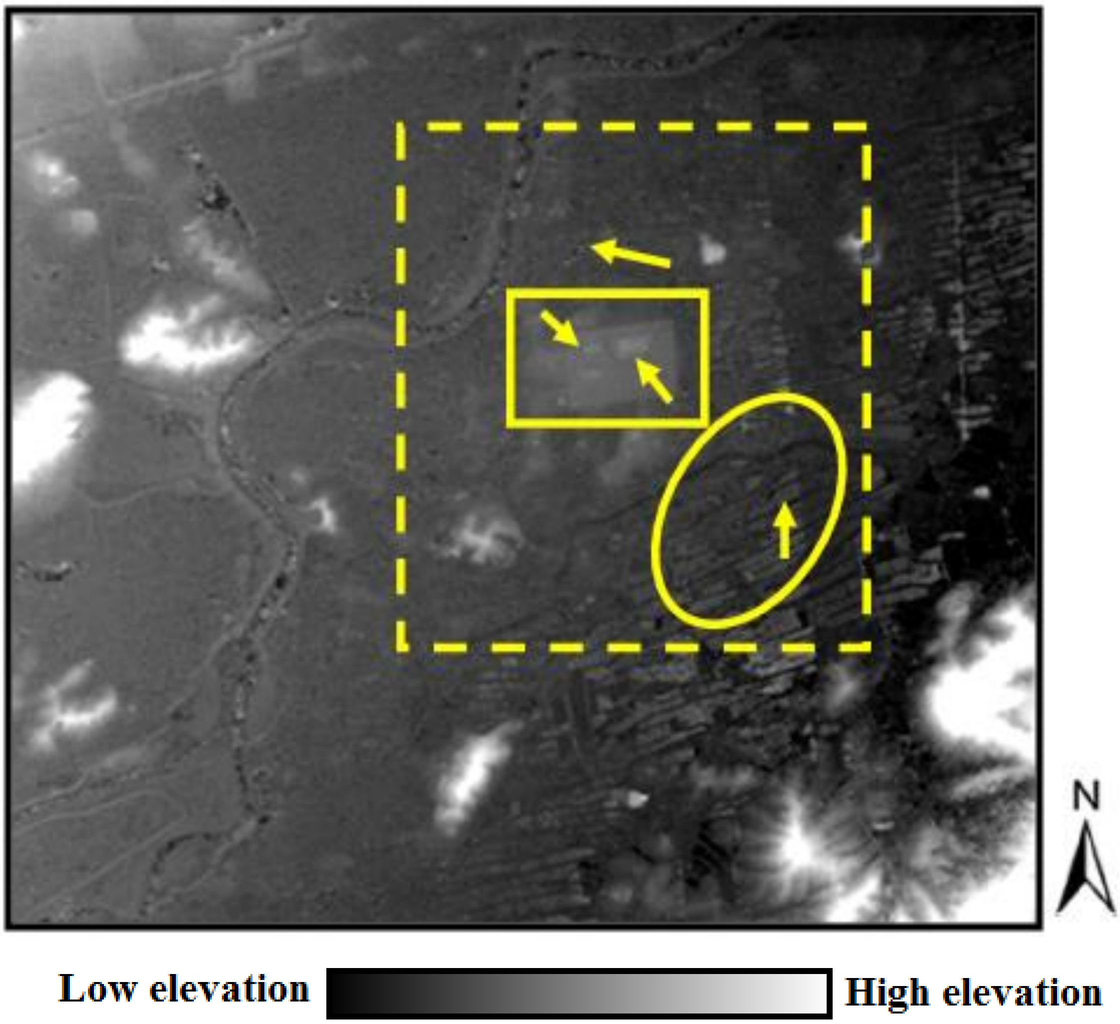

Figure 15. Estimated DSM imagery based UFSDSM over LAC. The yellow square, ellipse and arrows show representative archaeological sites. The square with yellow dash lines shows location of LAC. The coordinate centre of the image is 30°23′45″ N, 119°59′12″ E. The approximate spatial resolution of this image is 0.6-1.8m.

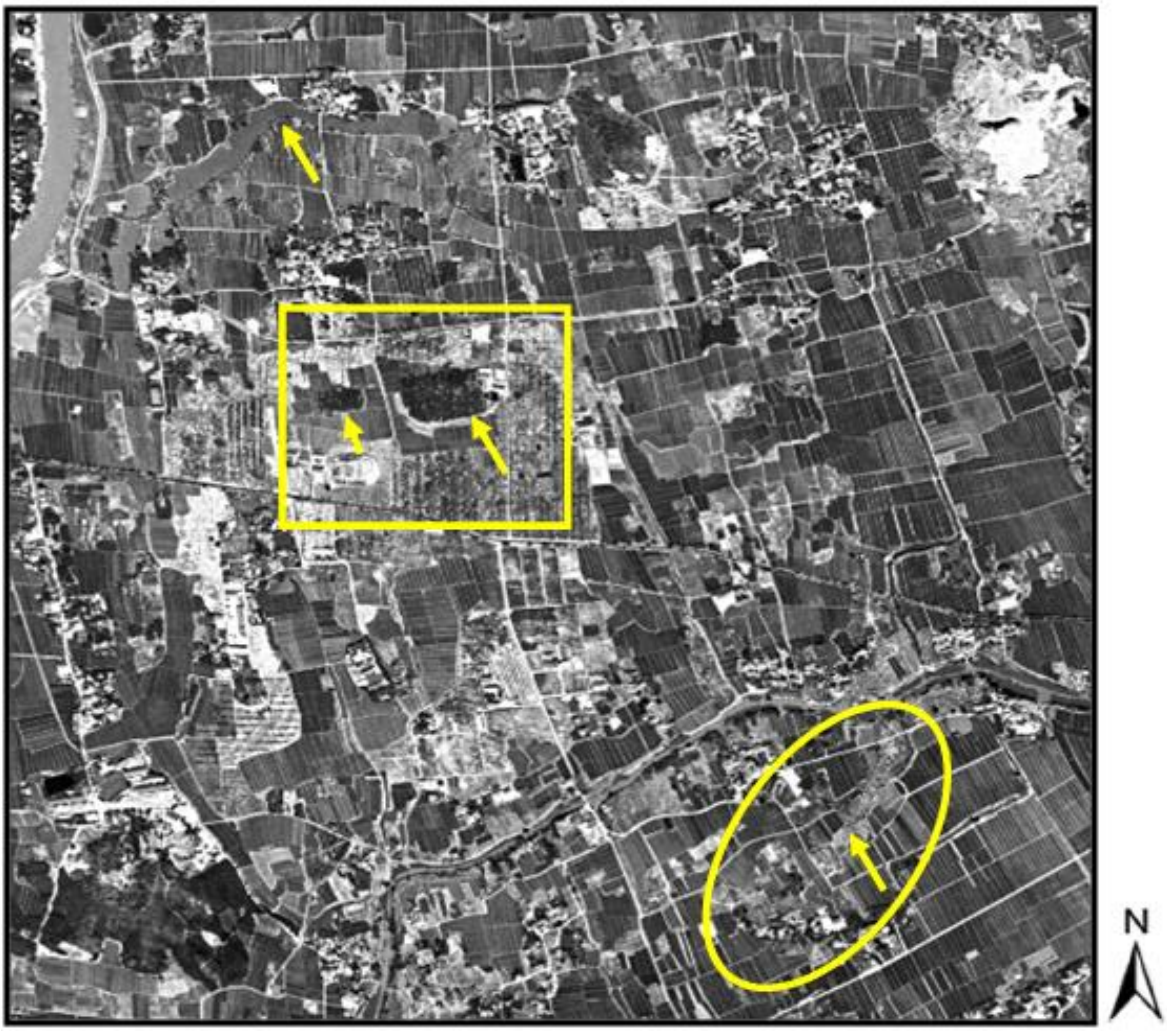

Figure 16. KH-9 PCS original image over LAC. The yellow square, ellipse and arrows show representative archaeological sites. The coordinate centre of the image is 30°23′45″ N, 119°59′12″ E. The approximate spatial resolution of this image is 0.6-1.8m.

4.4. Simultaneous analysing KH-9 PCS and MCS over LAC using proposed approaches

To have in-depth investigation, we also conducted joint analysis of the results of the proposed workflows for KH-9 PCS and MCS. Although KH-9 PCS image had finer spatial resolution in comparison with KH-9 MCS image, relying on a single panchromatic image either fine or medium spatial resolution may be insufficient for identifying archaeological features. The proposed workflows offered a useful and informative way to analyse such features. Interestingly, the obtained results by the proposed approached for KH-9 MCS (SCCWFM and SND) were supported by the finding of those for KH-9 PCS (stereo-pairs and DSM). For example, the SCCWFM image showed clearly the boundaries of a palace compound and its regular shape (Fig. 17(f): “A”, “B” and “C”) on the KH-9 MCS image. The abnormal variations in brightness values in this region were captured by SND (Fig.17 (e)). The shape and structures of this palace were depicted by UFSTCC (Figure.17(b)) and UFSDSM on KH-9 PCS (Figure.17(c)). In another example, the remains of a city wall can be identified easily on SCCWFM and SND (Fig. 18(e) and (f)). However, UFSTCC and UFSDSM revealed the details and micro-topography of this wall on KH-9 PCS (Figure. 18(b) and (c)).

(a) KH-9 PCS original **(b) KH-9 PCS, UFSTCC** **(c) KH-9 PCS , UFSDSM**

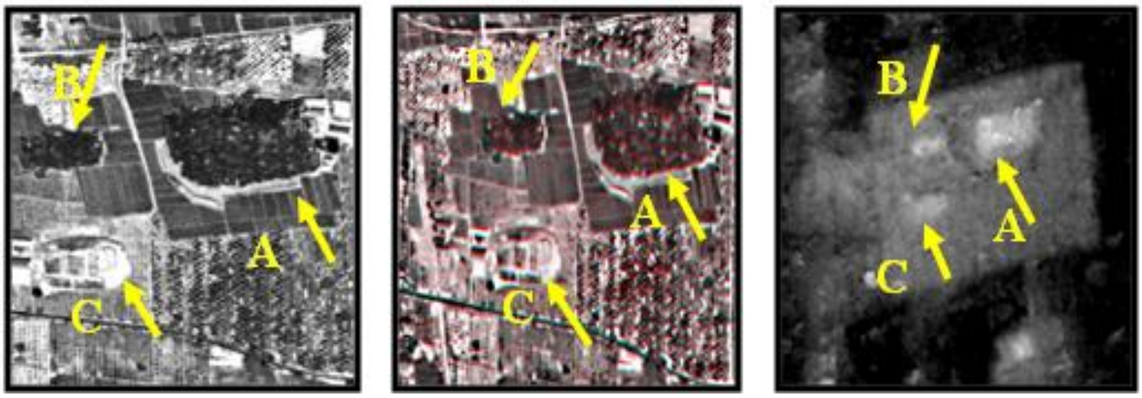

(d) KH-9 MCS original **(e) KH-9 MCS, SND** **(f) KH-9 MCS, SCCWFM**

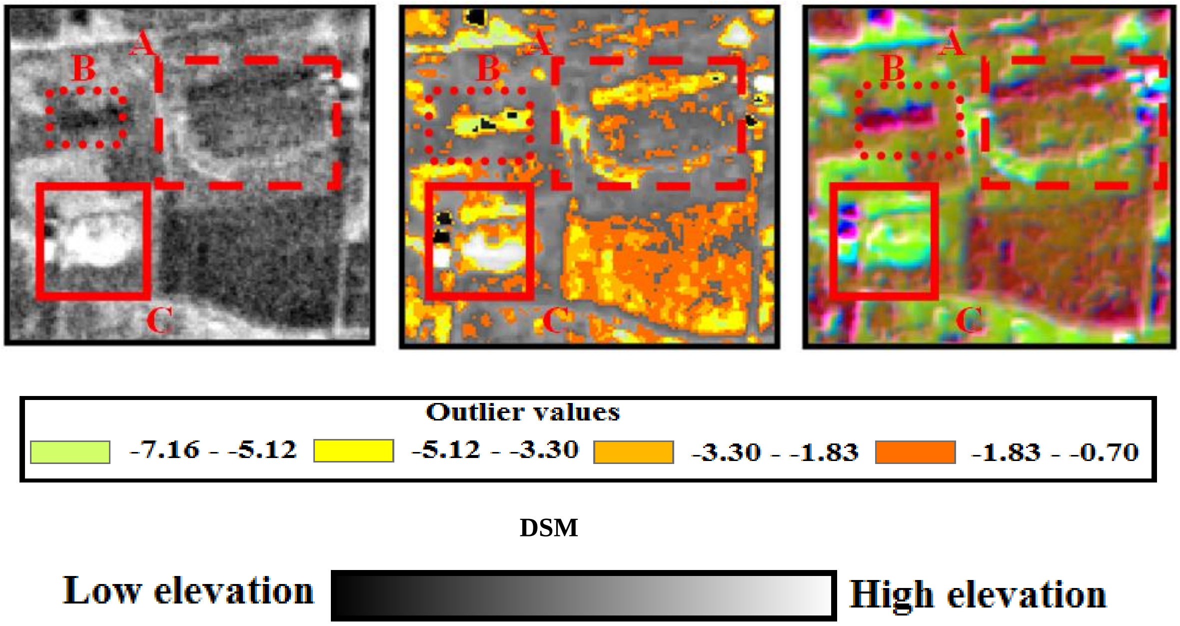

Figure 17. Joint analysis of KH-9 PCS and MCS products over palace compound in LAC region. The coordinate centres of images (a-c) and images (d-f) are 30°23′45″ N, 119°59′12″ E. The approximate spatial resolutions images (a-c) and images (d-f) are 0.6-1.8 and 6-9m, respectively.

(a) KH-9 PCS original **(b) KH-9 PCS,** UFSTCC (c) KH-9 PCS, UFSDSM

(d) KH-9 MCS original (e) KH-9 MCS, SND (f) KH-9 MCS, SCCWFM

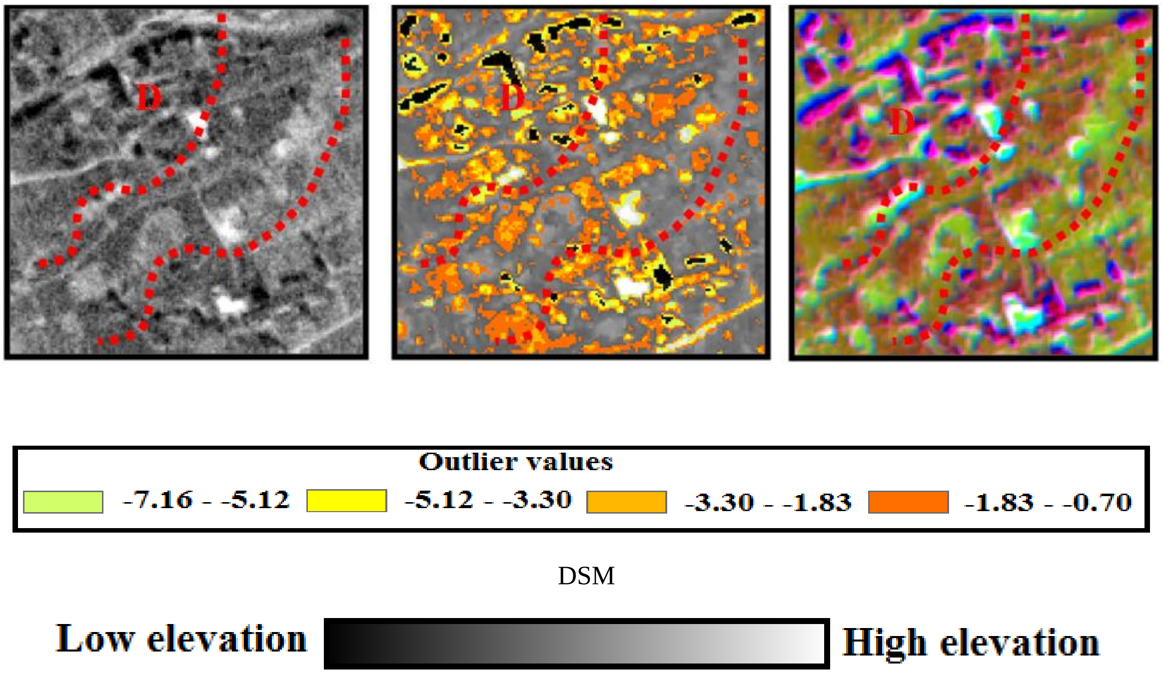

Figure 18. Joint analysis of KH-9 PCS and MCS products over southern part of the wall in LAC region. . The coordinate centres of images (a-c) and images (d-f) are is 30°23′18″ N, 119°59′40″ E. The approximate spatial resolutions images (a-c) and images (d-f) are 0.6-1.8 and 6-9m, respectively.

5. Discussion

5.1. Methodological implications

5.1.1. Pre-processing framework

Our research suggested that the original panchromatic imagery from KH-9 MCS and PCS may limit the precision of identifying archaeological features due to noise and brightness anomalies. It was demonstrated through the experiment conducted in this research that implementing a de-noising and contrast enhancement framework such as that developed here can enhance the quality of the KH-9 PCS and MCS imagery substantially and enable identification of archaeological features.

In terms of de-noising, although benchmark pre-processing algorithms based on the local spatial information showed some improvements above an original panchromatic image, they generated disappointing outcomes partly due to the lack of multi-resolution procedures and partly due to the lack of appropriate training. The proposed SWTNS approach not only enhanced the quality of the KH-9 PCS and MCS images across the targeted archaeological landscape, but also preserved the fine-scale details of image objects in comparison with the benchmark methods. The proposed SWTNS approach employed normalized sill (NS) which is based on the local spatial characteristics of the image brightness values. The NS acted as a useful supervised guide to selecting appropriate wavelet directional coefficients so as to simultaneously minimise the effects of noise, mitigate over- and under-smoothing and preserve the original image characteristics. Moreover, SWT benefited from multi-resolution procedure which considered spatial variation of the noise at the multiple scales (Wang, Istepanian, and Yong Hua 2003).

With respect to the contrast enhancement step, the proposed MTH enhanced appearance of the KH-9 MCS and PCS to the benchmarks. In fact, MTH used selective optimisation of local contrast by relationship between each pixel and its surrounding neighbourhood through shape and size of SEs at multiple scales, thus, preserving the characteristics of image details (Soille 2003).

Considering assessing performance of image pre-processing plays an overriding concern in remote sensing of archaeology, it is necessary to gauge precisely any changes to spatial characteristics of brightness values within the pre-processed image. This is because archaeological remote sensing relies heavily on image contrast for identifying features and their marks (Lasaponara and Masini 2007), thus, any alterations within the image may have a negative effect in subsequent procedures. In this view, conventional image quality assessment (e.g., Structural similarity index (SSIM)), may not provide comprehensive and systematic information for this issue. Therefore, this research proposed a suite of image quality assessment metrics based on the GLCM textures. Since these metrics adopted spatial neighbourhood, they present the response of the KH-9 PCS and MCS in details, in terms of local variations (contrast measure), spatial variation (variance measure), disorder (entropy measure) and distribution in the pixel pairs population (homogeneity measure), relative to alternative image pre-processing algorithms. Each measure of the GLCM provides comprehensive information about to which degree quality of image improved or degraded (Hall-Beyer 2017).

5.1.2. KH-9 MCS- SCCWFM and SND

To analyse archaeological landscape captured by KH-9 MCS image, we devised an approach with two components: qualitative and quantitative. The qualitative component composed of SCCWFM which employed textures, morphology, spatial, and edges of image objects. The proposed SCCWFM not only offered a colour composite image, but also it was sensitive to the spatial, edge and geometric characteristics of the image objects. Focusing on quantitative step, we proposed spatial novelty detection (SND) technique to map archaeological features. Bearing in mind, abnormal variation of brightness values (BVs) in archaeological remote sensing is highly important for identifying archaeological markers, thus, quantifying their corresponding archaeological features. The devised SND benefited from spatial neighbourhood and training procedure which helped to map spatial distribution of abnormal BVs from the KH-9 MCS imagery. Both qualitative (SCCWFM) and quantitative (SND) components added informatics and intelligent information for analysing KH-9 MCS imagery against a single panchromatic band.

5.1.3. KH-9 PCS- UFSTCC and UFSDSM

Lack of technical parameters of KH-9 PCS cameras, more importantly RPC coefficients, is one of the most important concerns for creating three-dimensional ultra fine spatial colour composite (UFSTCC) image and reconstructing ultra fine spatial digital surface model (UFSDSM). However, KH-9 PCS imagery offers ultra fine-scale textures in which state-of-the-art SfM approaches may benefit from this advantage. In terms of UFSTCC, the proposed three-dimensional technique matched two KH-9 PCS stereo images automatically using

Speeded-Up Robust Features (SURF) algorithm which is based on local spatial information. Moreover, our approach estimated camera parameters and projection by developed SfM algorithm in Matlab® (MathWorks Inc., Natrick, MA, USA. Release: 2022b). With respect to UFSDSM, we adopted SfM algorithm in Photoscan (Agisoft) software. The focal length and scan resolution were the only parameters for feeding this algorithm. Moreover, the adopted algorithm employed advances in computer-vision for image matching techniques which depends on ultra-fine scale textures. Both UFSTCC and UFSDSM were conducted full automatically. In contrast to the single panchromatic of KH-9 PCS, our investigation showed that UFSTCC provided a colour composite image with ultra fine-scale details and three-dimensional view while UFSDSM reconstructed DSM of study area at the very fine spatial resolution. It is safe to say that both UFSTCC and UFSDSM added a new dimension to our knowledge regarding Liangzhu archaeological landscapes prior to the current urbanisation in this region.

5.1.4. Software issues

One may ask " Are archaeologists or cultural heritage experts able to develop the proposed multifaceted approach or similar techniques?" Indeed, our research exploited advantages of contemporary spatial statistics and computer vision software. For example, python offers a scikit-learn package which includes a range of advanced machine learning techniques (Pedregosa et al. 2011). Of which, we adopted SND technique for mapping brightness anomalies on KH-9 MCS image. Additionally, Matlab® (MathWorks Inc., Natrick, MA, USA. Release: 2022b) consists of fully automatic SfM algorithm to reconstruct three-dimensional image (Anaglyph) from uncalibrated image. Thus, it is important to realise that using this software or similar one can make a considerable contribution to exploit the archaeological information latent in both KH-9 MCS and PCS imagery.

5.1.5. Challenges and recommendations

Despite the above promising outcomes, this research faced some challenges which should be addressed in future investigations. These challenges and potential recommendations are as follows:

(1) Wavelet transform depends only on three directions (i.e. vertical, horizontal and diagonal) which might not identify noise in every direction. Curvelet transform can be an alternative approach to tackle this problem as it takes into account every direction in the image. Moreover, wavelet transform and benchmarks techniques relied on interference of users for tuning parameters. Hence, future research may consider other automatic techniques such as deep learning for image de-noising.

(2) Although proposed approaches for KH-9 PCS and MCS provided promising performances, it is important to examine performance of advanced methods in image processing such as deep learning for reconstructing DSM, deep learning unsupervised classification and Gabor filter.

(3) This research did not deal with geometric distortion in KH-9 PCS and MCS images (Surazakov and Aizen 2010). This is because relaxing geometric distortion could have a direct effect on spatial and appearance of the image due to the several procedures within geometric corrections such as modelling image and resampling (Mather and Koch 2011; Morgan, Gergel, and Coops 2010). Therefore, the issue of geometric correction of these images for archaeological purposes should be addressed in future research.

(4) Considering availability of local reference information, we selected the LAC region which is located in a subtropical climate and is highly heterogeneous, comprising the juxtaposition of a mixture of archaeological remains, moist soil, vegetation covers, water bodies (such as rivers and ponds) and rural regions. Future investigation should assess

application of the proposed framework and KH-9 images in other landscapes particularly arid conditions.

(5) The proposed analytical framework for KH-9 data enhanced, extracted and mapped pattern, spatial distribution and micro-topography of archaeological remains in the LAC region. Such information can be integrated in designing polices for preservation and protection of cultural heritage sites, thus, ensuring that such region or other cultural heritage sites are respected. However, of particular note is that relaying only on KH-9 data could be insufficient for implementing such strategies. Hence, incorporating KH-9 data and the proposed framework with contemporary remotely sensed data can generate fine-scale spatio-temporal information of cultural heritage sites which can be utilised for sustainable management of these invaluable sites and respecting those regions.

(6) Obtaining high spatial resolution topographic data, conducting field campaign and acquiring GPS data were problematic in the study area (Watanabe et al. 2017). Such data play an overarching role for determining spatial, pattern and height of archaeological features in the LAC region. To tackle such problems, this research utilised Google Earth^{TM} images and cross-referencing. Future research may exploit advantages of other open access data sources such as open street map, ASTER GDEM images and ALOS World 3D data.

(7) In order to comprehensively understand patterns of archaeological features in LAC from KH-9 images, we recommend integration of KH-9 images with other archaeological data sources, such as site plans, excavation reports, and other satellite or aerial imagery. Such comparisons could also pave the way to implement appropriate archaeological and cultural protection policies.

(8) This research utilised the Local Outlier Factor (LOF) algorithm which characterises novel pattern based on the analysing spatial relationships. Further research is needed to assess performance of other geospatial analysis techniques (such as local Moran’s I, local Geary’s C and Getis–Ord local Gi) using geographic information systems (GIS) to analyse spatial relationships, patterns, and distributions among the identified archaeological features from KH-9 images.

5.2. Interpreting LAC landscape using proposed multifaceted analytical approach

In the main, the most distinguishing objects of archaeological landscapes from remotely sensed data are crop marks and soil marks (Lasaponara and Masini 2007). Therefore, image object parameters such as tone, texture, shape, shadow, geometry, and elevation can be used for such marks (Fowler and Fowler 2005). However, identifying these marks based on a single panchromatic band under a subtropical climate with heterogeneous landscape types is non-trivial task (Watanabe et al. 2017).

The use of the proposed multi-component processing enabled us to improve the identification of diverse buried archaeological features in LAC. The proposed SCCWFM and SND revealed that the LAC consisted of a complex and heterogeneous surface due to the presence of many geometric features. In this view, UFSTCC showed the details of LAC in which this site can be divided into two categories: non-archaeological category such as farmlands which were mirrored by homogeneous surfaces and archaeological category which were reflected by heterogeneous surfaces due to presence of many geometric features. Moreover, UFSDSM revealed structure archaeological remains in the LAC such as the main palace in its centre. Comparison between our results and previous research (Watanabe et al. 2017; Yu et al. 2018) suggested that the proposed methodology is capable to accurately verify previous findings with fewer challenges, as mentioned in former studies. This is because the proposed feature identification framework offers two major advantages: (1) SCCWFM and SND are sensitive to feature properties (shape, geometry) and brightness anomalies, respectively; and (2) UFSTCC and UFSDSM paves the way to highlight quantitatively details and structure of archaeological features within three-dimensional view in the LAC.

Along with previously discovered features (Watanabe et al. 2017; Yu et al. 2018), SCCWFM, SND, UFSTCC and UFSDSM showed many unknown features in the LAC. These features formed discontinuous patches with curvilinear shapes which could suggest the presence of archaeological remains. This finding is concordant with the results of previous studies (e.g.,Lasaponara et al. 2016; Lasaponara et al. 2018) which demonstrated that the existence of geometric features and spatial discontinuities due to pattern anomalies may be indicators of ancient human activities. Moreover, these characteristics could be supported by Landscape Mosaic Theory (LMT) which shows that spatial discontinuities across a landscape may reflect remains of human activity patches as they have experienced rapid and abrupt changes in contrast to natural patches (Forman 1995). However, further archaeological investigation needs to be carried out to assess this finding.

It is noteworthy that a previous research on KH-9 PCS imagery suggested that creating digital elevation model (DEM) or DSM based on this imagery could contribute to identifying archaeological features, and revealing their structures (Hammer, FitzPatrick, and Ur 2022). Indeed, our findings also supported this suggestion in which generated DSM by the proposed method detected archaeological remains in LAC, and quantified their shape and structure. Also the proposed DSM was consistent with reference DSM which was produced by aerial photography (Figure 19) (Zhejiang_Provincial_Institute_of_Cultural_Relics_and_Archaeology 2015). Hence, future archaeological research may exploit advantages of DEM/DSM based KH-9 PCS imagery.

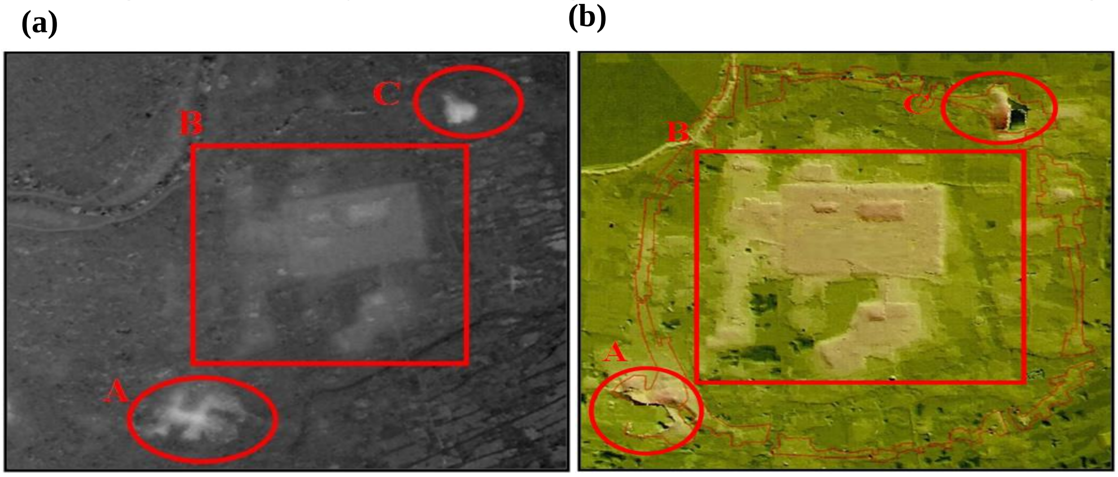

Figure 19. DSM over LAC site, comparison between (a) generated DSM using proposed framework and (b) reference DSM by aerial photograph
(edited from the DSM map of Zhejiang_Provincial_Institute_of_Cultural_Relics_and_Archaeology (2015))
The coordinate centre of the images (a) and (b) is 30°23′45″ N, 119°59′12″ E. The approximate spatial resolution of the image (a) is 0.6-1.8m.

5.3. Capability of KH-9 satellite images for Archaeological studies

We have demonstrated that well pre-processed images (i.e., de-noising and contrast enhancement) of KH-9 images can offer archaeologists and other scientists a remote assessment tool so as to develop a baseline to analyze past conditions of archaeological landscapes. We have also shown that developing appropriate feature identification framework (i.e., SCCWFM, SND, UFSTCC and UFSDSM) based on the state-of-the-art in digital image processing can facilitate identification of archaeological features on both KH-9 PCS and MCS panchromatic images.

All these facts indicate that KH-9 imagery can be widely used in archaeological investigations in 1970s and can offer fine-scale details of archaeological remains. Ultimately, investing on proposing analytical approaches (i.e., pre-processing and feature identification) for declassified KH-9 imagery may have great potential to support attainment of the United Nations Sustainable Development Goals (Luo et al., 2019), such as developing a remote sensing archaeological baseline. To achieve the 17 SDGs, the UN emphasizes that "…we call for increased support for strengthening data collection and capacity building in Member States, to develop national and global baselines where they do not yet exist...." (United_Nation 2015). Considering availability of worldwide imagery at fine spatial scales, processed KH-9 imagery could also provide fundamental information for each archaeological site, and thus support archaeological protection projects such as the Endangered Archaeology in the Middle East and North Africa (EAMENA) project (https://eamena.org). To achieve such goals, future archaeological studies based on KH-9 images should pay more attention to applications of existing or developing new digital analytical pipelines, particularly for dealing with large volumes of images necessary for studying larger archaeological regions.

.

6. Conclusion

This research has aimed to highlight the unique possibilities for analysing fine-scale archaeological landscapes offered by declassified KH-9 PCS and MCS panchromatic images, particularly when used in the subtropical climate regions in which landscapes are highly heterogeneous, comprising the juxtaposition of a mixture of archaeological remains, moist soil, vegetation covers, water bodies (such as rivers and ponds) and other land cover types. Such landscapes can lead to mixed pixels among different land cover types from a single panchromatic band. For instance, surfaces such as water, moist soil, archaeological remains and vegetation covers may exhibit very similar values in panchromatic imagery, resulting in misinterpretation errors. In addition, existing noise and contrast distortions in KH-9 images impede accuracy of both visual interpretation and digital image processing. Particularly, heterogeneity of landscapes can be increased by noise and contrast distortions in the image. Ultimately, we demonstrated the feasibility of developing a multi-stage pipeline to tackle these problems. The developed approach included two components: image pre-processing and feature identification. The efficiency of this approach was scrutinized at an ancient landscape, Liangzhu Ancient City, as representative of archaeological landscapes under subtropical climate with heterogeneous landscape. The pre-processing component was able to convert the original scanned KH-9 MCS and PCS images into distortion-free (de-noised and optimized contrast) images by means of SWT and MTH. In terms of feature identification, the information produced by proposed analytical approaches can inform investigators about past conditions of archaeological regions (e.g., the type of sites, their distribution, micro-topographic reliefs and relationship to their surroundings) prior to any land use changes. Additionally, careful investigation based on the above techniques revealed many unknown features with some distinctive characteristics: (1) straight boundaries, (2) discontinuous patches, (3) micro-topographic relief and (4) curvilinear shapes. These characteristics could lead to greater clarity on the past conditions (i.e., highly heterogeneous) of Liangzhou Ancient City (LAC).

Considering the availability of worldwide KH-9 images at fine spatial scales, investing on proposing analytical approaches (i.e., pre-processing and feature identification) for declassified KH-9 imagery not only could support attainment of the United Nations Sustainable Development Goals (such as 17 SDGs), but also developing spatial database using KH-9 images could facilitate protection and management of archaeological and cultural heritage sites such as Endangered Archaeology in the Middle East and North Africa (EAMENA) project (https://eamena.org). Therefore, we identify the following recommendations for future research:

1) In order to develop KH-9 database, future research should assess other image pre-processing techniques (such as deep learning) and feature identification approaches

particularly based on geospatial analysis using GIS , state-of-the-art in machine learning and artificial intelligent (AI).

2) Establishing multi-source database using contemporary remotely sensed data, field surveys, historical map and KH-9 images so as to monitor comprehensively conditions of archaeological and cultural sites (such as unchanged and damages) with respect to urbanisation, agricultural development, looting, conflicts, natural disaster and other potential threats, thus implementing and mitigating appropriate regulations.
3) Raising awareness of the capability of KH-9 images and providing training courses for utilising such images in archaeological contexts among archaeological researchers, practitioners and managers as well as many disciplines that employ historical remotely sensed imagery in their research.

The KH-9 archive represents a unique repository for remote sensing of archaeology. It is hoped that this research paves the way for more research on digital processing of the KH-9 archive and encourages its use in archaeological investigations.

Declaration of interests

No potential conflict of interest was reported by the authors.

Acknowledgements

We thank the Editors and anonymous reviewers for their very constructive comments.

References

Aubry, M., S. Paris, S. W. Hasinoff, J. Kautz, and F. Durand. 2014. "Fast Local Laplacian Filters: Theory and Applications." *Acm Transactions on Graphics* 33 (5). doi: 10.1145/2629645.

Bai, X. Z., F. G. Zhou, and B. D. Xue. 2012. "Image enhancement using multi scale image features extracted by top-hat transform." *Optics and Laser Technology* 44 (2):328-36. doi: 10.1016/j.optlastec.2011.07.009.

Breunig, M. M., H. P. Kriegel, R. T. Ng, and J. Sander. 2000. " LOF: identifying density-based local outliers." In *Proceedings of the 2000 ACM SIGMOD International Conference on Management of Dat*. Dallas, Texas, USA.: In ACM sigmod record.

Casana, J. 2020. "Global-scale archaeological prospection using CORONA satellite imagery: automated, crowd-sourced, and expert-led approaches." *Journal of Field Archaeology* 45 89-100. doi: 10.1080/00934690.2020.1713285.

Dehecq, A., A.S. Gardner, O. Alexandrov, S. McMichael, R. Hugonnet, D. Shean, and M. Marty. 2020. "Automated Processing of Declassified KH-9 Hexagon Satellite Images for Global Elevation Change Analysis Since the 1970s." *Front. Earth Sci* 8 (566802). doi: 10.3389/feart.2020.566802.

Forman, Richard T. T. 1995. *Land mosaics : the ecology of landscapes and regions*. Cambridge ; New York: Cambridge University Press.

Fowler, M. 2016. "The archaeological potential of declassified HEXAGON KH-9 panoramic camera satellite photographs." *AARG News* 53:30-6.

———. 2022. "The archaeological potential of KH-9 HEXAGON satellite photographs: the Roman temporary camps and siege works at Machaerus and Masada." *AARG News* 64:37-53.

Fowler, M.J.F. 2013. "Declassified Intelligence Satellite Photographs. ." In *Archaeology from Historical Aerial and Satellite Archives*, edited by W. Hanson and I. Oltean. New York, NY: Springer.

Fowler, M.J.F. , and Y.M. Fowler. 2005. "Detection of Archaeological Crop Marks on Declassified CORONA KH-4B Intelligence Satellite Photography of Southern England." *Archaeological Prospection* 12:257-64 doi: 10.1002/arp.266.

Galiatsatos, N. . 2004. " Assessment of the CORONA Series of Satellite Imagery for Landscape Archaeology: A

Case Study from the Orontes Valley, Syria." Durham.

Galiatsatos, N., D.N.M. Donoghue, and G. Philip. 2008. "High resolution elevation data derived from stereoscopic CORONA imagery with minimal ground control: an approach using Ikonos and SRTM data. ." *Photogramm. Eng. Remote. Sens.* 74 (9):1093–106.

Hall-Beyer, M. 2017. "Practical guidelines for choosing GLCM textures to use in landscape classification tasks over a range of moderate spatial scales." *International Journal of Remote Sensing* 38 (5):1312-38. doi: 10.1080/01431161.2016.1278314.

Hammer, E . , M. FitzPatrick, and J. Ur. 2022. "Succeeding CORONA: declassified HEXAGON intelligence imagery for archaeological and historical research." *Antiquity* 96 , Issue 387 , June 2022 , pp. (387): 679 - 95. doi: 10.15184/aqy.2022.22.

Jensen, John R. 2005. *Introductory digital image processing : a remote sensing perspective*. 3rd ed, *Prentice Hall series in geographic information science*. Upper Saddle River, N.J.: Prentice Hall.

Lasaponara, R., G. Leucci, N. Masini, R. Persico, and G. Scardozzi. 2016. "Towards an operative use of remote sensing for exploring the past using satellite data: The case study of Hierapolis (Turkey)." *Remote Sensing of Environment* 174:148-64. doi: 10.1016/j.rse.2015.12.016.

Lasaponara, R., and N. Masini. 2007. "Detection of archaeological crop marks by using satellite QuickBird multispectral imagery." *Journal of Archaeological Science* 34 214-21. doi: 10.1016/j.jas.2006.04.014.

———. 2011. "Satellite remote sensing in archaeology: past, present and future perspectives." *Journal of Archaeological Science* 38

1995–2002. doi: 10.1016/j.jas.2011.02.002.

Lasaponara, R., R. X. Yang, F. L. Chen, X. Li, and N. Masini. 2018. "Corona Satellite Pictures for Archaeological Studies: A Review and Application to the Lost Forbidden City of the Han-Wei Dynasties." *Surveys in Geophysics* 39 (6):1303-22. doi: 10.1007/s10712-018-9490-2.

Luo, L., X. Y. Wang, H. D. Guo, R. Lasaponara, X. Zong, N. Masini, G. Z. Wang, et al. 2019. "Airborne and spaceborne remote sensing for archaeological and cultural heritage applications: A review of the century (1907-2017)." *Remote Sensing of Environment* 232.

Marzolff, I. , M. Kirchhoff, R. Stephan, M. Seeger, A. Aït Hssaine, and JB. Ries. 2022. "Monitoring Dryland Trees With Remote Sensing. Part A: Beyond CORONA-Historical HEXAGON Satellite Imagery as a New Data Source for Mapping Open-Canopy Woodlands on the Tree Level." *Front. Environ. Sci* 10:896702. doi: 10.3389/fenvs.2022.896702.

Mather, Paul M., and Magaly Koch. 2004. *Computer processing of remotely sensed images : an introduction*. 3rd ed. Chichester, West Sussex, England ; Hoboken, NJ: John Wiley & Sons.

Mather, Paul M., and Magaly. Koch. 2011. *Computer processing of remotely sensed images : an introduction*. 4th ed. Chichester, West Sussex, England ; Hoboken, NJ: John Wiley & Sons.

Maurer, J., and S. Rupper. 2015. "Tapping into the Hexagon spy imagery database: A new automated pipeline for geomorphic change detection." *Isprs Journal of Photogrammetry and Remote Sensing* 108:113-27. doi: 10.1016/j.isprsjprs.2015.06.008.

Morgan, J. L., S. E. Gergel, and N. C. Coops. 2010. "Aerial Photography: A Rapidly Evolving Tool for Ecological Management." *Bioscience* 60 (1):47-59. doi: 10.1525/bio.2010.60.1.9.

Nita, M. D., C. Munteanu, G. Gutman, I. V. Abrudan, and V. C. Radeloff. 2018. "Widespread forest cutting in the aftermath of World War II captured by broad-scale historical Corona spy satellite photography." *Remote Sensing of Environment* 204:322-32. doi: 10.1016/j.rse.2017.10.021.

Pedregosa, F., G. Varoquaux, A. Gramfort, V. Michel, B. Thirion, O. Grisel, M. Blondel, et al. 2011.

"Scikit-learn: Machine Learning in Python,.,." *Journal of Machine Learning Research* 12:2825-30.

Scardozzi, G. 2010. "The contribution of historical aerial and satellite photos to archaeological and geo-archaeological research: case studies in Italy and Turkey." *Advances in Geosciences* 24:111–23. doi: 10.5194/adgeo-24-111-2010.

Shahtahmassebi, A.R., M. Liu, L. Li, J. Wu, M. Zhao, X. Chen, L. Jiang, et al. 2023. "De-noised and contrast enhanced KH-9 HEXAGON mapping and panoramic camera images for urban research,." *Science of Remote Sensing* 7. doi: 10.1016/j.srs.2023.100082.

Soille, Pierre. 2003. *Morphological image analysis : principles and applications*. 2nd ed. Berlin ; New York: Springer.

Surazakov, A., and V. Aizen. 2010. "Positional Accuracy Evaluation of Declassified Hexagon KH-9 Mapping Camera Imagery." *Photogrammetric Engineering and Remote Sensing* 76 (5):603-8. doi: Doi 10.14358/Pers.76.5.603.

United_Nation. 2015. " "Transforming our world: the 2030 Agenda for Sustainable Development " " In.

Ur, J. 2003. "CORONA satellite photography and ancient road networks: a northern Mesopotamian case study." *Antiquity* 77:102–15. doi: 10.1017/S0003598X00061391.

Wang, X. H., R. S. H. Istepanian, and Song Yong Hua. 2003. "Microarray image enhancement by denoising using stationary wavelet transform." *IEEE Transactions on Nanobioscience* 2 (4):184-9. doi: 10.1109/tnb.2003.816225.

Wang, Y., W.J. Huang, Y.Q. Han, X.D. Huang, C. Wang, K.X. Ma, M.Y. Kong, N. Jiang, and J. Pan. 2022. "Microbial diversity of archaeological ruins of Liangzhu City and its correlation with environmental factors " *International Biodeterioration & Biodegradation* 175. doi: 10.1016/j.ibiod.2022.105501.

Watanabe, N., S. Nakamura, B. Liu, and N. Y. Wang. 2017. "Utilization of Structure from Motion for processing CORONA satellite images: Application to mapping and interpretation of archaeological features in Liangzhu Culture, China." *Archaeological Research in Asia* 11:38-50. doi: 10.1016/j.ara.2017.06.001.

Yu, L. J., Y. Zhang, Y. P. Nie, W. J. Zhang, H. G. Gao, X. Y. Bai, F. Liu, Y. Hategekimana, and J. F. Zhu. 2018. "Improved detection of archaeological features using multi-source data in geographically diverse capital city sites." *Journal of Cultural Heritage* 33:145-58. doi: 10.1016/j.culher.2018.01.001.

Zhejiang_Provincial_Institute_of_Cultural_Relics_and_Archaeology. 2015. "The detection of the outer city of the Liangzhu ancient city and the excavations of the Meirendi and Biandanshan sites in Hangzhou." In *Kaogu (Archaeology)*, 3-13.